

Beta-prototype of a Rickshaw Suspension System

by

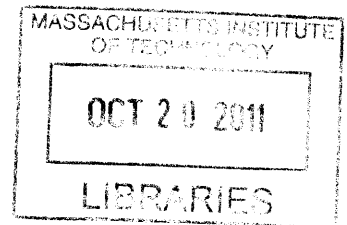
Heather E. McDonald

Submitted to the Department of Mechanical Engineering  
in Partial Fulfillment of the Requirements for the  
Degree of

Bachelor of Science

at the

Massachusetts Institute of Technology  
June 2011



ARCHIVES

© 2011 Heather McDonald  
All rights reserved

The author hereby grants to MIT permission to reproduce and to distribute publicly paper and  
electronic copies of this thesis document in whole or in part in any medium now known or  
hereafter created.

*Handwritten signature of Heather E. McDonald*

Signature of Author

.....  
Department of Mechanical Engineering  
May 6, 2011

*Handwritten initials*

Certified by: .....

*Handwritten signature of Barbara Hughey*

Barbara Hughey  
Instructor of Mechanical Engineering  
Thesis Supervisor

Accepted by: .....

*Handwritten signature of John H. Lienhard V*

John H. Lienhard V  
Samuel C. Collins Professor of Mechanical Engineering  
Undergraduate Officer



Handwritten text, possibly a signature or a set of initials, located in the lower-left quadrant of the page. The text is very faint and difficult to decipher.

## Table of Contents

<b>Table of Contents</b> .....	<b>3</b>
<b>Nomenclature</b> .....	<b>4</b>
<b>Abstract</b> .....	<b>5</b>
<b>1 Introduction</b> .....	<b>7</b>
1.1 Motivation .....	7
1.1.1 The Rickshaw Bank: A Community Partner .....	7
1.2 Current Problems with Rickshaw Suspension .....	8
1.3 Constraints .....	9
1.4 Previous Work .....	10
1.4.1 Spring and Damper Systems .....	10
1.4.2 The Alpha-prototype .....	11
<b>2 Problem Statement</b> .....	<b>14</b>
<b>3 Beta-prototype Design</b> .....	<b>14</b>
3.1 Constraints and Requirements .....	14
3.2 Materials and Manufacturing Processes Used .....	15
<b>4 Theoretical Analysis: How Does The Beta-prototype Work?</b> .....	<b>16</b>
4.1 Spring Compression .....	16
4.2 Going Over A Bump .....	18
4.3 Parameters That Affect Performance .....	24
4.3.1 The Importance of Spring Stiffness .....	24
4.3.2 The Mount's Geometry .....	25
<b>5 Apparatus and Procedure</b> .....	<b>27</b>
5.1 Experimental Set-Up .....	28
5.2 Testing .....	29
5.3 Analysis Tools .....	29
5.4 Figure of Merit $\phi$ .....	33
<b>6 Testing Results and Discussion</b> .....	<b>33</b>
6.1 Finding India at MIT .....	34
6.2 Finding Appropriate Configuration .....	35
<b>7 Conclusion</b> .....	<b>42</b>
<b>Appendices</b> .....	<b>43</b>
Appendix A: Beta-prototype Dimensions .....	43
Appendix B: Tire Rubber Donut Manufacturing Instructions .....	50
Appendix C: From the Ground's Frame of Reference .....	51
Appendix D: MathCad Code .....	53
Appendix E: Additional Average Gain and $\phi$ Comparisons .....	60
<b>References</b> .....	<b>64</b>

## Nomenclature

$A_0$	original cross-sectional area of the tire rubber donut
$\alpha$	angle between the spring and the top link
$\beta$	angle between the spring and the front wheel axle bar
$c_i$	length of the vertical moment arm between position $i$ on the top link and the ground
$d$	diameter of tire rubber donuts
$E$	Young's Modulus
$\varepsilon$	engineering strain
$F$	force
$F_i$	force applied at point $i$ or by $i$ , as described in paper
$f$	frequency
$h$	distance from mount attachment on top link and the pivot between the top link and the front wheel axle bar
$\kappa$	standard deviation of $\varphi$
$L$	length of the entire stack of tire rubber donuts
$L_0$	original length of the entire stack of tire rubber donuts
$\Delta L$	change in length of the entire stack of tire rubber donuts
$\lambda_0$	original length of one tire rubber donut
$\Delta\lambda$	change in one tire rubber donut's length
$M$	moment
$n$	number of points taken within the frequency range
$\varphi$	figure of merit (the average of the average gain for a given configuration and frequency range)
$\phi$	uncertainty of $\varphi$
$\sigma$	engineering stress
$T$	period
$x$	length of moment arm
$x_s$	length of moment arm of perpendicular force of spring on the top link
$x_a$	length of moment arm of perpendicular force of the front wheel axle bar on the top link
$z_i$	length of the horizontal moment arm between position $i$ on the top link and the ground

# Beta-prototype of a Rickshaw Suspension System

by

Heather E. McDonald

Submitted to the Department of Mechanical Engineering  
on May 6, 2011 in Partial Fulfillment of the  
Requirements for the Degree of Bachelor of Science in  
Mechanical Engineering

## **Abstract**

A suspension system was designed to make The Rickshaw Bank's bicycle-powered rickshaws more comfortable for the drivers. A four bar linkage with a rising rate spring was chosen as the design. An unconventional material—tire rubber—was used as the spring material because it is inexpensive, requires limited tooling, and is in vast supply near The Rickshaw Bank's factory in Assam, India.

Different configurations of tire rubber were tested to see how the size, length, and placement of the spring affected the system's performance. Bode Plots of the system's response function were generated for each configuration. The functionality of the suspension system within the 10-20 Hz range was of premier importance because it is in this frequency range that the bicycle-powered rickshaws most often operate, based on their speed and the road conditions the rickshaw regularly encounters.

Ultimately, it was demonstrated that the placement of the spring within the suspension system had the greatest effect on the system's response. The configuration that applied the greatest moment to the top link of the four bar linkage performed best. Surprisingly, any advantages arising from varying the geometry of the tire rubber pieces were lost to friction and the effect of the ply embedded in the tire rubber.

In order to properly verify the optimal spring placement and tire rubber spring geometry, a suspension system that takes this paper's findings into account should be tested with a rickshaw in India.

Thesis Supervisor: Barbara Hughey  
Title: Instructor of Mechanical Engineering



## 1 Introduction

Since its invention hundreds of years ago, the rickshaw has been a staple form of transportation on many continents. A rickshaw, in its most generic form, is no more than a human-drawn, two-wheeled cart with a seat for passengers. Depending on the region, rickshaws are either pushed from behind or pulled from the front. Later iterations replaced the person walking with a person riding a bicycle, as illustrated in Figure 1. These tricycle-like rickshaws are very popular throughout southern and eastern Asia, especially with the middle and lower classes. This thesis will focus on the bicycle powered rickshaw most commonly used in India.



Figure 1: Bicycle-Pulled Rickshaws. Both photos, taken in India, show bicycle rickshaws carrying passengers.

### 1.1 Motivation

There are approximately 80 million rickshaws in India. Because of their slow pace (that of a human walking while bearing a heavy load), traditional rickshaws have been outlawed in almost all of India, leaving bicycle-pulled rickshaws as the vast majority of the 80 million rickshaws on the road today.

Over 95% of these rickshaws in India are not owned by the rickshaw drivers themselves. Rather, the drivers pay high daily rental fees, leaving little more than \$1 USD as their average nightly take-home pay. The drivers take care of any maintenance that the rickshaw needs and are held fiscally responsible if the rickshaw is damaged as part of a traffic accident.

On top of these monetary impediments, the drivers face the tough task that their livelihood provides for them. Indian rickshaws are not only called upon to pull the two people for which the seat was originally intended. Instead, these rickshaws carry anything from school children heading for class to loads of bricks for a new construction project. The often heavy loads, coupled with the difficult road and traffic conditions, take a heavy toll on the driver's body. Often drivers complain of pain in their elbows, knees, and ankles.

#### 1.1.1 The Rickshaw Bank: A Community Partner

These drivers' problems do not go completely unnoticed. In 2004, Dr. Pradip Sarmah created The Rickshaw Bank<sup>1</sup>, a nonprofit organization that specializes in reaching out to the marginalized urban poor. Located in Guwahati, the capital of the Indian state of Assam, this

nonprofit's main goal is to allow rickshaw drivers to own their own rickshaws, while raising the quality of life of the drivers and their families.

In order to accomplish this mission, The Rickshaw Bank uses a rent-to-own system. For the first 12-18 months, a rickshaw driver pays a smaller than normal daily rental fee. In exchange for this fee, he receives a rickshaw, a uniform, a photo identification card, and some free medical services for himself and his family at local partner hospitals. The Rickshaw Bank's rickshaws last about 5 years, allowing the drivers to earn significantly more money than they otherwise would have in the poverty perpetuating cycle of high daily rental fees with no hope of ownership. The Rickshaw Bank raises the capital for what basically amount to high risk loans via corporate sponsorship. This nonprofit's rickshaws, shown in Figure 2, were designed such that the back of each rickshaw is a large, moving billboard. Banks and businesses throughout Guwahati can pay to permanently advertise their goods or services on the back of a particular rickshaw.



Figure 2: The Rickshaw Bank's Rickshaws. In this photo<sup>2</sup>, several of The Rickshaw Bank's rickshaws are waiting for passengers. The back of each rickshaw has an advertisement for a local bank or business.

Dr. Pradip Sarmah wishes to further increase the drivers' quality of life by improving the rickshaw on which they spend much of their day. With this in mind, he approached D-lab staff member Gwyn Jones in 2008. Through this partnership, new designs have been made to make the rickshaw lighter, cheaper, and easier to ride. Of specific interest is the quest to make the rickshaw relatively easier to ride.

### **1.2 Current Problems with Rickshaw Suspension**

The joint pain experienced by rickshaw drivers is largely due to the rough road conditions. Currently, rickshaws used throughout India protect only the passengers from the extremely bumpy roads through either coiled springs in the seat cushions or a suspension system using steel leaf springs between the seat and the rear axle. The drivers are left exposed.

A driver will often be straining to pull his load up a countryside hill or along at the slow crawl of inner-city traffic. When the rickshaw's front wheel suddenly plunges into a deep rut, his tensed arm and leg muscles act as ridged bars, leaving his joints to absorb the brunt of the impact. The drivers' bodies are constantly subjected to these large impulses as they spend 12-14 hour workdays towing their passengers and freight over the pothole-riddled roads.



In summation, the main problem with rickshaw suspension is that there is none available for the drivers. Over time, the strong impulses take a toll on the drivers' bodies, rendering them unable to work. Therefore the total earning capability of the person is decreased by the rapid deterioration of his joints, shortening not only his livelihood, but also his life.

### **1.3 Constraints**

The drivers could certainly benefit from a suspension system on the front fork of the rickshaw. However, there are many barriers to the construction of an acceptable system. Besides working properly, the suspension system must be designed to cost as little as possible while using locally available materials and simple tooling. The system must also fit neatly into the drivers' current perception of a good, sturdy fork.

Because The Rickshaw Bank is working to make rickshaw ownership within reach of the common man, the cost to manufacture each rickshaw is extremely important. Currently, each rickshaw costs \$220 USD. A price increase of 10% would add approximately another two months onto the rickshaw driver's payment schedule. Therefore, Dr. Sarmah requested that the suspension fork cost no more than an additional \$10 for materials and labor. Manual labor in Guwahati is very cheap, so the main focus for the rickshaw suspension system must be to avoid introducing any unusually expensive components as part of the design.

Using locally available materials is an effective way to keep the cost of the suspension system low. The current rickshaw design consists primarily of one inch diameter tubing and angle iron. While many other materials are readily available at local markets, it makes the most sense to utilize the materials that are already purchased for the factory. The local markets also often lack the variety necessary to find a specific material, so any design must not hinge on a very particularly sized component, but rather be flexible to allow construction with available materials. For example, while rod may always be available, the diameter of the cheapest rod will fluctuate as market prices change to adjust to supply chain inefficiencies.

The rickshaw factory itself is not a factory by American standards. Besides being the small one room bamboo building pictured in Figure 3, the tooling is quite limited. At the factory in Guwahati, there are two welders, a low torque drill press, a circular saw, an electric grinder, and a variety of hand tools. Therefore, the suspension system must not rely on extremely precise clearances or have very strict tolerances. While the men who work in the factory are experts, it would be wrong to ask them to create something that is far outside the scope of their tooling's capabilities.



Figure 3: The Rickshaw Bank Factory. Though not a factory by any American standards, the workers at the factory build all of The Rickshaw Bank's rickshaws by hand. In the background, one can see a man sitting at the low torque drill and another grinding the rough edges of a weld on a rickshaw frame. The man kneeling on the right edge of the picture is currently welding part of a rickshaw frame.

Finally, the suspension system must be aesthetically pleasing to the drivers. Regardless of how many calculations or tests that have been done to prove that the system will not fail, if it looks too unstable or unusual, drivers will not be willing to pay extra for a feature that they've been told will help them. Money is too precious a commodity to be wasted on something that looks awkward or unwieldy. The best way to ensure driver acceptance is to make the suspension system look similar to the current front forks on the market.

#### **1.4 Previous Work**

In the Fall of 2009, Gwyn Jones began teaching a class called "Cycle Ventures," which spent much of its time focusing on designing and building a better rickshaw. In this class, the alpha-prototype of the suspension system was created\*.

##### **1.4.1 Spring and Damper Systems**

Over the history of bicycles, there have been many different forms of suspension. Today's mountain bikes feature a hydraulic spring and damper system. This provides great suspension for the rider as she travels down a rocky mountain hill, making it seem ideal for the road conditions in Guwahati. However, this suspension system would not be suitable for Indian rickshaws for several reasons. First, it is too expensive to purchase outright. To fabricate it in The Rickshaw Bank's factory would be too difficult because of the extremely small clearances that allow the hydraulic damper to function. Third and most importantly, the energy lost to

---

\* The alpha-prototype was designed by four students at MIT: Madeline Hickman, James Jenkins, Heather McDonald, and Angharad Porteous.

damping is simply too great. The drivers value their momentum more than even their own comfort. This is evident in their tires, which are filled to the maximum allowable air pressure and often beyond. Had they filled the tires within the appropriate range, the tires would provide some cushion against the rough roads. Yet, in order to decrease the amount of rolling friction, the drivers fill their tires to the maximum, gaining only a small advantage in terms of frictional losses for a rather sizable loss in terms of comfort.

Another system, similar to a motorcycle suspension, was proposed by the Indian Institute of Technology several years ago<sup>3</sup>. The IIT design mounted springs along the original bicycle fork, such that the front wheel axle telescoped towards or away from the handlebars. This configuration compressed when the drivers actually hit the bump, only to spring back unexpectedly as soon as the bump had been cleared. Drivers complained that these systems were worse than driving without a suspension system at all.

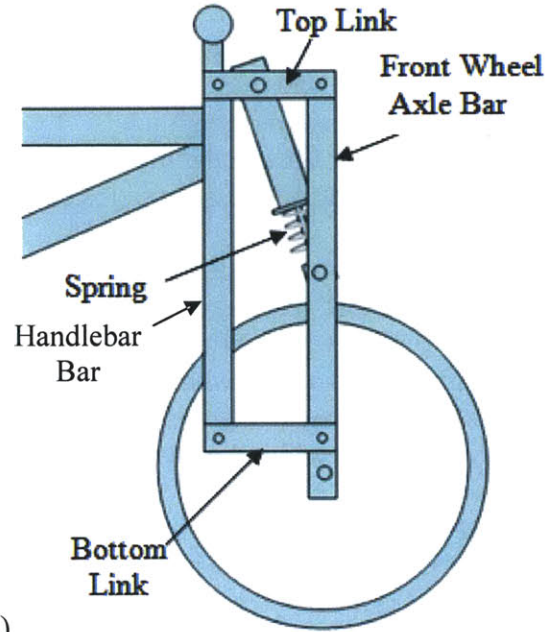
#### **1.4.2 The Alpha-prototype**

A four bar mechanism is the basic structure for the alpha-prototype because it is simple to construct and can easily be built with the one inch tubing that is prevalently used in the rickshaw's current design. Using a material with a proven strength is a critical part of the rickshaw drivers' acceptance of the new system. The structure is made of two identical halves, a left and a right side which are joined together by several rods so that they will operate in tandem. One side of the suspension fork will be described here.

The structure, which can be seen in Figure 4, is set up such that one of the bars is long and connected to the front wheel axle. Another bar of a similar length is connected to the handlebars and the steer tube. These two bars are connected by two links: one at the top, just below the handlebars; and the other at the bottom, just above the front wheel axle. This system will allow the front wheel axle to move independently of the handlebars for a given length, based on the geometry of the four bar linkage.



(a)



(b)

Figure 4: The Alpha-prototype. (a) This photo was taken shortly after the alpha-prototype was assembled and attached to a rickshaw at The Rickshaw Bank factory. Because the left vertical support was made from a straightened bike fork, it had to be further supported by making it into a triangular truss. (b) This is a simplified diagram of the alpha-prototype. Every circle in the diagram is a pivot point. The details of the spring and mount are shown in Figure 5.

In order to provide the spring and damper system, one compression spring is centered between the two halves of the suspension fork's structure. The compression spring is attached to the center of the front wheel axle bar and to the center of the top link. This configuration, shown in Figure 5, provides a rising spring rate. A spring with a rising spring rate becomes stiffer as it is compressed, while a standard spring's stiffness does not change as it is compressed. While the spring itself is a standard compression spring, the configuration is such that as the spring is compressed, it behaves like a spring with a rising spring rate. Therefore, using a spring in this configuration allows the suspension system to move a shorter distance for a given force, relative to the amount that a different configuration without a rising spring rate would move. The spring's configuration within the alpha-prototype allows the overall frame to be smaller (because it needn't move as far) than it otherwise might have been to accommodate similar sized bumps. The rising spring rate also provides a sort of natural damping, never allowing the spring to simply jump back to its initial position.

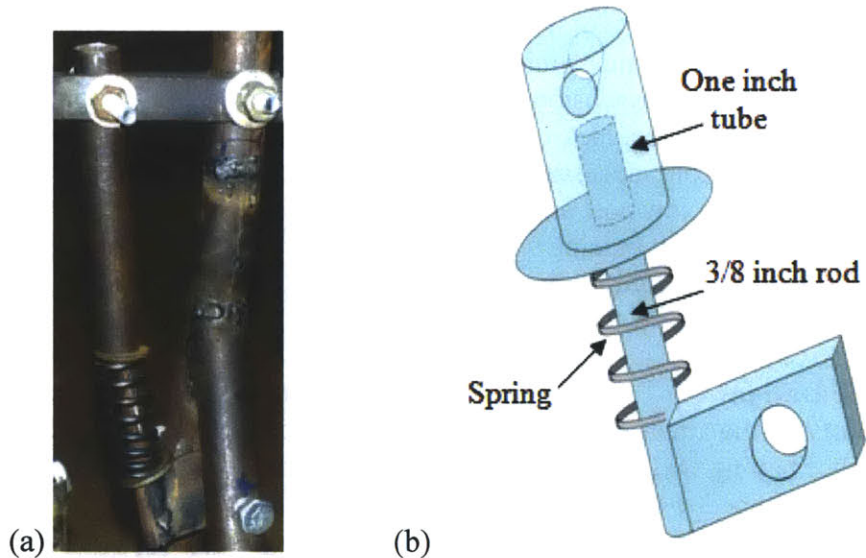


Figure 5: Alpha-prototype Spring Mount. (a) This is a photograph of part of the alpha-prototype's suspension system. The bar on the right hand side connects to the front wheel axle below the picture's frame. The top link connects to the handlebar bar just off the left edge of the frame. (b) This sketch shows how the spring is mounted into the system. The rod is allowed to move freely within the piece of one inch tubing. When the rod is forced up into the tube by the movement of the suspension system, the spring is compressed.

In order to hold the spring in this configuration, a special mount was developed. The side of a 3/8 inch diameter rod was butt-welded to an edge of a rectangular piece of steel. The compression spring was then slid onto the rod between two washers. A piece of one inch diameter tubing was slid onto the rod after the spring. The rectangular piece of steel was then mounted onto a rod that linked the twin front wheel axle bars at their center. The piece of one inch diameter tubing was attached to another rod that connected the two top links, so that these would also move in tandem. Both the rectangular piece of steel and the one inch diameter tubing were allowed to pivot at these attachments.

This version was built at The Rickshaw Bank's factory in Guwahati in January 2010 by members of the Cycle Ventures class\* with the help of the instructor Gwyn Jones and The Rickshaw Bank factory workers. During the process of building the alpha-prototype, a major problem was encountered. While the four bar mechanism worked well, the group had trouble finding an appropriately stiff spring. Only small toy springs and large motorcycle springs were available at the local markets. In order to test the system, a spring of inadequate stiffness was used. It became coil-bound† when a person of approximately 125 pounds sat on the driver's seat but was able to move slightly before becoming coil-bound when a local man weighing about 100 pounds sat in the driver's seat. In spite of these difficulties, it was qualitatively demonstrated that the design did decrease the impact felt when driving the rickshaw over fairly small bumps.

\* Heather McDonald and Angharad Porteous fabricated the prototype in Assam.

† When a spring becomes coil bound, it has been compressed to the point where all of the coils in the spring are touching one another. Because there are no longer any gaps between the coils, the spring cannot compress any further.

## 2 Problem Statement

It has been shown that a four bar mechanism with an appropriately placed compression spring is a viable option for a rickshaw suspension system. However, the spring and damper system has not been fully operational due to a lack of locally available steel compression springs of the proper stiffness. It is, therefore, necessary to explore other avenues for the spring material. This new material will need to be low cost and locally available. The design that will hold it in the appropriate position to maintain a rising spring rate must be within the capability of The Rickshaw Bank's factory's limited tooling.

## 3 Beta-prototype Design

For the beta-prototype, the alpha-prototype's structure was slightly altered, in order to use less material. Instead of having two equally sized bars on both the front wheel axle and the handlebars, the bar attached to the handlebars was shortened, so that it is barely lower than the bottom of the steer tube, as shown in Figure 6. The bottom link now travels from the bottom of the steer tube to a point along the front wheel axle bar, remaining approximately parallel with the top link. Also, the spring mount was changed slightly. The lower attachment point is now inline with the spring, rather than being welded such that it is off center. Fully dimensioned drawings of the system can be found in Appendix A.

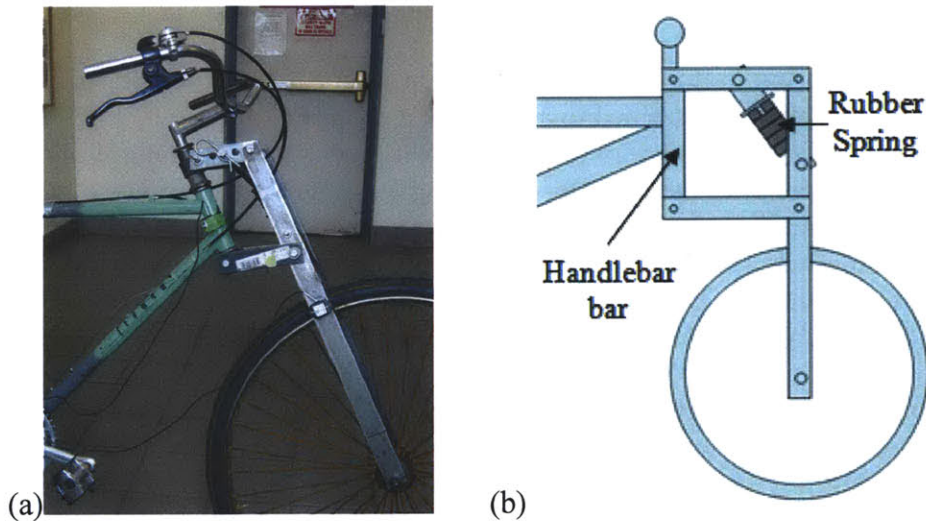


Figure 6: Beta-prototype. (a) This photograph of the beta-prototype shows the suspension system in an uncompressed form. The bar attached to the handlebars has been shortened, relative to the alpha-prototype. (b) This diagram of the beta-prototype allows easier viewing of the structural changes.

### 3.1 Constraints and Requirements

The new spring material must be low cost and locally available and the mount for holding the new spring in place must be able to be manufactured at The Rickshaw Bank's factory.

The stiffness required of the spring must match the loading experienced by the front wheel of the rickshaw. The normal load experienced by the front wheel of the rickshaw is predominantly only the weight of the person peddling the rickshaw. This is because, in The Rickshaw Bank's rickshaw design, the weight of the passengers or goods is centered over the back axle.

Therefore, the back axle bears the vast majority of the weight of the additional passengers. Because of this weight distribution, it is unnecessary for the spring stiffness to be tolerant of a wide range of loading conditions, since the weight on the front wheel is only a function of the driver's weight. However, a given configuration should tolerate a range of driver weights, as rickshaw drivers can vary from boys in the early teens to full grown men. It would be beneficial but not necessary to design a suspension system that can be adjusted for the weight of a specific rickshaw driver.

### 3.2 Materials and Manufacturing Processes Used

Directly next door to The Rickshaw Bank's factory is a garage that works on triple axle trucks. Piles of worn tires are heaped at the garage, awaiting disposal. This tire rubber, given rubber's elasticity, could potentially be used as the spring material. Unlike the steel belted radial tires<sup>4</sup> found on American cars today, these Indian tires are bias ply tires. A bias ply tire is a tire that contains inextensible threads (called ply) embedded into the rubber of tire. The ply, most commonly made from polyester cord<sup>5</sup>, is set in an overlapping weave pattern, providing extra strength for the tire. Figure 7 illustrates one possible configuration for the ply.

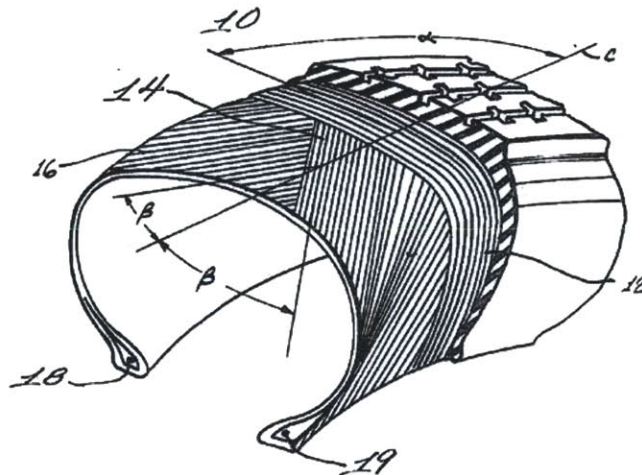


Figure 7: Cutaway diagram of a car tire<sup>6</sup>. The items that are numbered fourteen and sixteen are the bias ply. Number twelve shows the radial ply. Both are normally employed in the bias ply tires found in India.

Pieces of the tire's sidewall could readily be used as a compression spring if they were stacked on top of one another. In order to prepare the tire pieces to be easily mounted in a stacked configuration, the tire was cut into donut shapes using a hole saw\*, like the tire rubber donut pictured in Figure 8. The tire rubber donuts were then slid onto a 3/8 inch rod in approximately the same location as the alpha-prototype's steel compression spring. For detailed directions on creating the tire rubber donuts, see Appendix B.

\* A hole saw is a standard attachment to a power drill.



Figure 8: Tire Rubber Donut. The top of the tire rubber donut shown in the photo is the outside of the sidewall of the tire. The fibers near the bottom are the threads that compose the ply.

#### 4 Theoretical Analysis: How Does The Beta-prototype Work?

The entire premise of this suspension system design is that it is theoretically possible for the front wheel and the handlebars to move independently of one another. Before diving into how exactly the suspension system as a whole functions, it is critical to first understand spring compression.

##### 4.1 Spring Compression

Imagine that an external force is applied to both ends of the suspension system's spring. This external force is equally spread across the entire cross-sectional area of each tire rubber donut, assuming that the washers on either end of the tire rubber donut stack are at least as large as the tire rubber donuts and that the diameter of the stacked tire rubber donuts is uniform. If these conditions are not met, the forces will not be equally distributed across the faces of the tire rubber donuts. However, the basic operating principles outlined below still apply. Figure 9 shows one tire rubber donut just as an external force  $F$  is beginning to be applied to it.

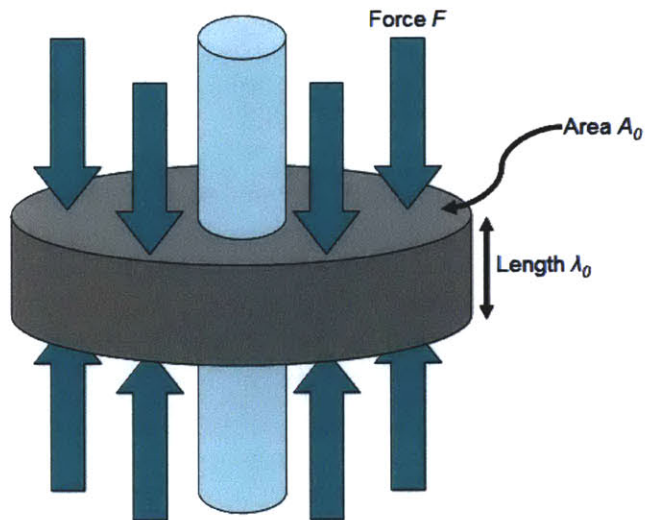


Figure 9: Tire Rubber Donut Experiences an External Force. This diagram shows a tire rubber donut with an uncompressed cross-sectional area  $A_0$  and an uncompressed length  $\lambda_0$  being subjected to some force  $F$  which is equally distributed across both faces of the tire rubber donut.



The tire rubber donut will continue to compress until the force exerted by the compressed tire rubber is equal to the externally applied force. At this point, the forces are said to be balanced and the system is in equilibrium. Ultimately, the force exerted by the compressed spring is based on the amount of strain experienced by the material. Strain is induced when the spring changes shape. Engineering strain  $\varepsilon$  can be calculated, using Equation (1), based on measurements taken before external forces are applied and at the point of interest (often at the some equilibrium point).

$$\varepsilon = \frac{\Delta\lambda}{\lambda_0}, \quad (1)$$

where  $\lambda_0$  is the original length of one tire rubber donut and  $\Delta\lambda$  is the change in one tire rubber donut's length.

Engineering stress  $\sigma$  is directly related to engineering strain through the material's Young's Modulus, as demonstrated in Equation (2). Young's Modulus  $E$  is an intrinsic physical property of a material that quantifies the stiffness of the material. For the tire rubber donuts, the Young's Modulus is unknown and difficult to quantify due to the ply threads embedded in the material.

$$\sigma = E\varepsilon \quad (2)$$

Engineering stress can then be used to calculate the force exerted by the compressed spring  $F$ . As Equation (3) shows, only the original cross-sectional area  $A_0$  is needed to calculate the engineering stress, given the force the spring must apply.

$$\sigma = \frac{F}{A_0} \quad (3)$$

The force of the spring material can then be expressed in terms of the spring material's geometry and intrinsic property, as in Equation (4).

$$F = \frac{EA_0 \Delta\lambda}{\lambda_0} \quad (4)$$

While this derivation has been done for a single tire rubber donut, it is readily applied to the entire length of the stack of tire rubber donuts. The total compressive spring force can then be written as shown:

$$F = \frac{EA_0 \Delta L}{L_0}, \quad (5)$$

where  $L_0$  is the original length of the entire stack of tire rubber donuts and  $\Delta L$  is the change in length of the entire stack of tire rubber donuts.

The amount that the entire spring material compresses  $\Delta L$  can be referred to as the system's *travel*.

## 4.2 Going Over A Bump

When an external force from a bump is applied to the suspension system, the four bar linkage moves because the forces are no longer in balance. Unbalanced forces cause acceleration to occur in the direction of the net force. In equilibrium, forces on any given element of the system must be in balance vertically, horizontally, and angularly. The angular forces are referred to as moments. Equations (6a-c) mathematically lay out all of these equilibrium conditions.

$$\Sigma F_{vertical} = 0, \quad (6a)$$

$$\Sigma F_{horizontal} = 0, \text{ and} \quad (6b)$$

$$\Sigma M = \Sigma x_i F_i = 0, \quad (6c)$$

where  $\Sigma F_{vertical}$  is the summation of all vertical forces,  $\Sigma F_{horizontal}$  is the summation of all horizontal forces,  $\Sigma M$  is the summation of all moments,  $x_i$  the distance away from a given pivot point that a force acts—known as the moment arm, and  $F_i$  is the force acting perpendicular to the moment arm.

If the forces are unbalanced in the horizontal or vertical directions, the entire piece will translate in the direction of the net force. If the moments are unbalanced, the element will pivot around the fixed point on the system, much like the arms of a seesaw pivot around the center.

In order to best understand how the system generally functions, examine Figure 10.

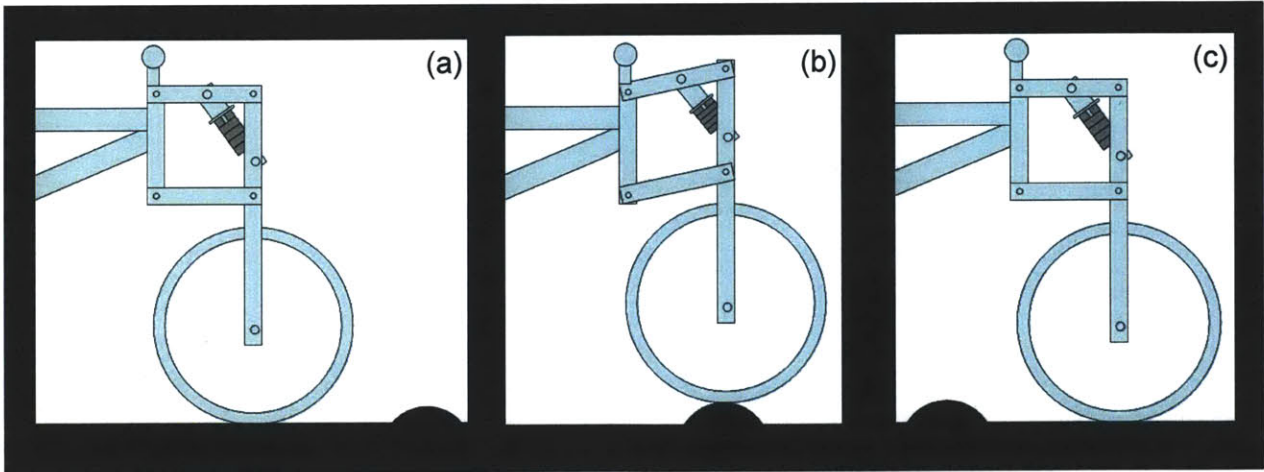


Figure 10: Riding Over a Bump. This comic strip details the idealistic operation of the suspension system. (a) The rickshaw approaches a bump. (b) As the rickshaw rides over the bump, the bar attached to the front wheel axle rises while the handlebars stay in the same position. The spring is compressed. (c) Having cleared the bump, the compressed spring goes back to its original shape. Throughout the entire ride, the handlebars remain in the same location.

The suspension system's entire functionality can be described in detail by focusing on two elements of the system: the front wheel axle bar and the top link. By examining in detail the forces applied to and the motion of these elements throughout one loading cycle—that is, while the bicycle rides over one bump—the physics governing the system as a whole can be well understood. As illustrated in Figure 11, the dimensions of interest are the moment arm of the perpendicular force of the spring on the top link  $x_s$ , the moment arm of the force from the front

wheel axle bar  $x_a$ , the angle between the spring and the top link  $\alpha$ , and the angle between the spring and the front wheel axle bar  $\beta$ . The following explanation will be given from the reference frame of the handlebars\* .

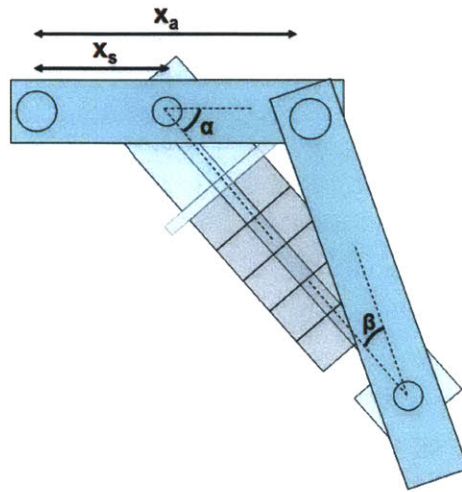


Figure 11: The Dimensions of Interest. The moment arm of the perpendicular force of the spring on the top link  $x_s$ , the moment arm of the force from the front wheel axle  $x_a$ , the angle between the spring and the top link  $\alpha$ , and the angle between the spring and the front wheel axle bar  $\beta$  are shown in the diagram.

The first force balance of interest is the balancing of the forces along the length of the front wheel axle bar as described by Equation (6a). This direction, though not exactly vertical, will be referred to as vertical hereafter because it is nearly a vertical motion. The front wheel axle bar is constrained to move in only the vertical direction because it is attached to both the top and bottom links. These links are in turn attached to pivots on the handlebar bar. Therefore, the entire bicycle would need to move in order to accommodate a horizontal or angular movement of the front wheel axle.

The second force balance of interest involves the top link. The top link is constrained to move only angularly relative to the handlebars, which are the frame of reference. The leftmost pivot is part of the fixed reference frame and cannot translate in the vertical or horizontal directions. Therefore, the force balance on this element will actually be a moment balance. For this moment balance, all forces acting along the length of the top link will not be mentioned because they act parallel to the moment arm and are therefore not relevant.

---

\* While determining exactly how the handlebars move while riding over a bump is out of the scope of this paper, the governing equations and free body diagram necessary to solve that problem are located in Appendix C. Those equations use the ground as a reference frame.

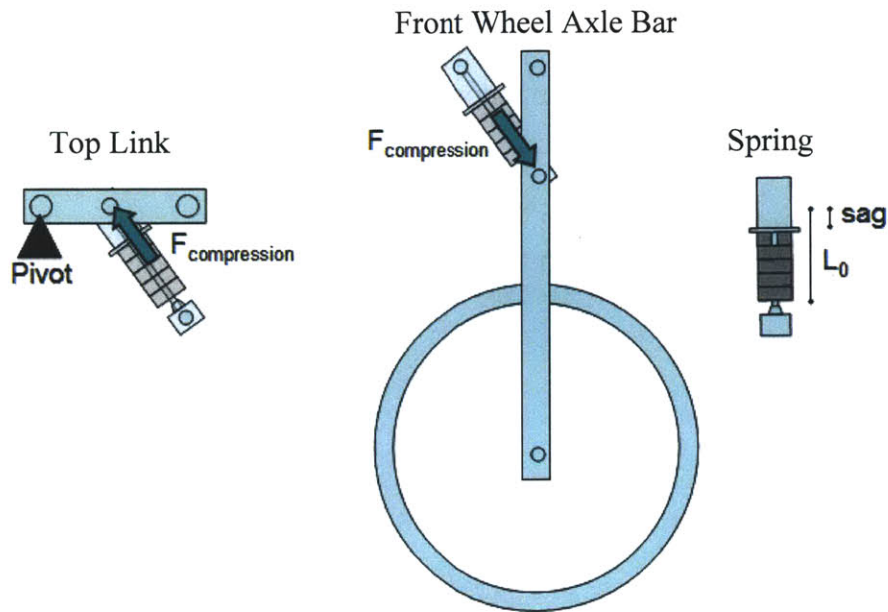


Figure 12: Before The Spring Strikes A Bump. The two elements of interest as well as the spring are shown in their neutral positions.  $F_{\text{compression}}$  is the force exerted by the spring as it is compressed. The amount that the spring has been compressed is called *sag*. The uncompressed spring has a length  $L_0$ .

Before the spring strikes a bump, the suspension system is in equilibrium, as shown in Figure 12. The weight of the suspension fork, the bicycle portion of rickshaw, and the rickshaw driver are balanced by the force of the slightly compressed spring. The amount of that the spring is compressed in these loading conditions is called *sag*. Please note: For the rest of this explanation, the force due to the weight of the bicycle will be ignored for simplicity's sake.

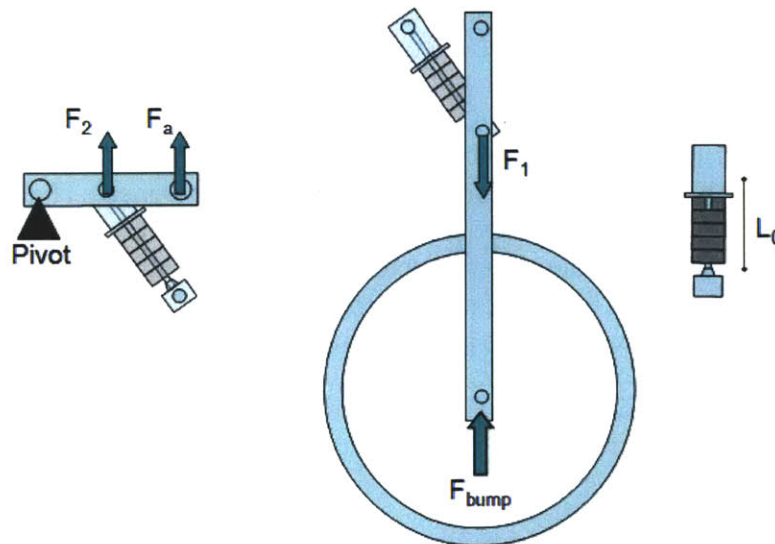


Figure 13: The Suspension System Hits A Bump. The top link, the front wheel axle bar, and the spring are shown. The force of the bump will cause both elements to become unbalanced.  $F_1$  is the force along the length of the front wheel axle bar due to the compression of the spring,  $F_2$  is the portion of the spring's compressive force that is exerted on the top link perpendicular to the moment arm,  $F_a$  is the force exerted by the front wheel axle bar on the top link perpendicular to the moment arm, and  $F_{\text{bump}}$  is the force provided by the bump.

When the suspension system first hits the bump, the force of the bump is transferred from the front wheel to the front wheel axle to the front wheel axle bar with very few losses. (The only loss would occur if the tire was filled such that it absorbed some of the bump's energy as though it was a spring.) The force, shown in Figure 13, from this bump is initially greater than the force on the spring, causing the front wheel axle bar to accelerate vertically.

The vertical acceleration of the front wheel axle bar applies a force to the top link seen in Figure 13. This force, partnered with the force of the compressed spring (due to sag), causes the top link to rotate around the pivot point. The top link has an angular acceleration because of the moment imbalance.

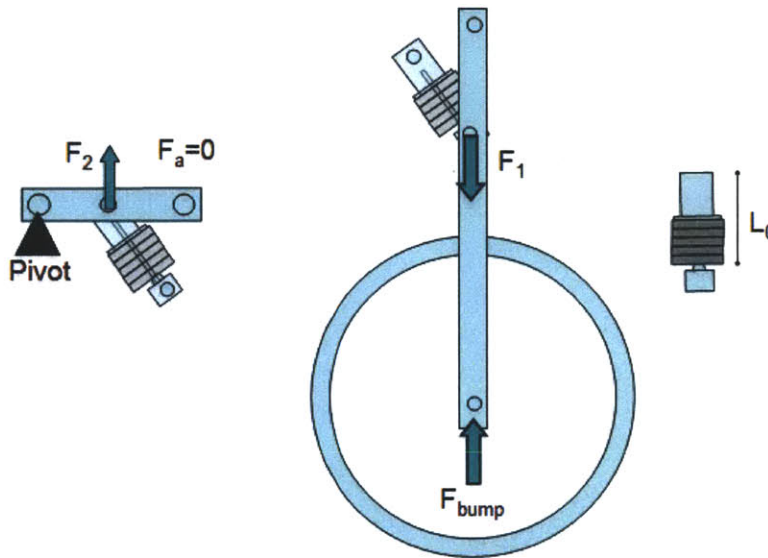


Figure 14: The Front Wheel Axle Bar's Forces Balance. The forces on the front wheel axle bar are balanced momentarily. The instantaneous acceleration in the vertical direction is zero for the front wheel axle bar.

The vertical acceleration of the front wheel axle and the angular acceleration of the top link are greatest the instant the force from the bump is applied. As the spring is further compressed, the vertical component of the spring force felt by the front wheel axle bar increases. At the instant shown in Figure 14, the vertical components of the force of the bump and the force of the spring are equal. At that moment, the front wheel axle bar stops accelerating. However, it still does have momentum, which continues to carry it in the positive vertical direction.

The top link is still accelerating angularly. As the front wheel axle bar rises, the force of the spring on the top link increases for two reasons. First, the compression of the spring causes the overall compressive spring force to increase. Second, the motion of the top link as it pivots around the leftmost pivot causes the angle between the spring and the top link to approach  $90^\circ$ , thereby increasing the percentage of the spring's force that acts perpendicularly to the top link.

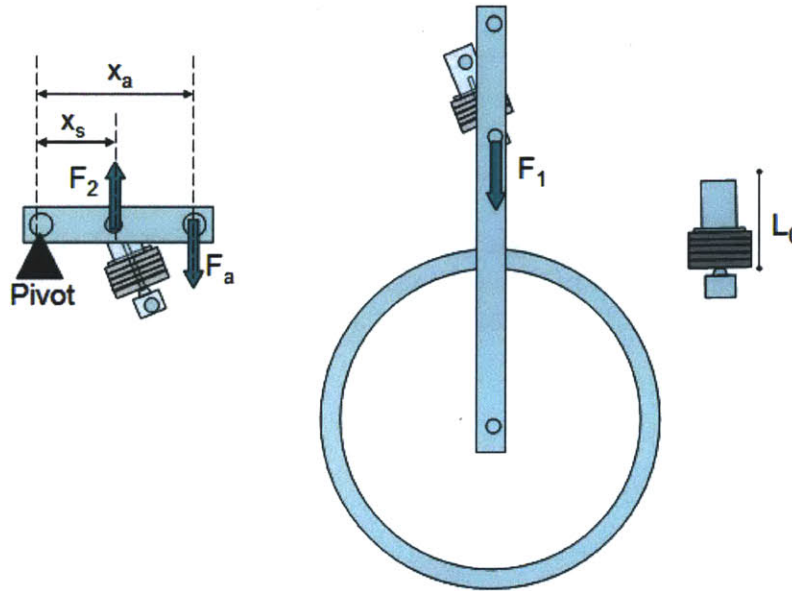


Figure 15: Top Link's Moments Balance. The moment balance on the top link is zero.

The front wheel axle bar begins to decelerate as the force of the spring becomes greater than the force of the bump. The front wheel axle bar's velocity in the positive vertical direction begins to decrease. Because the force of the spring is greater than the force of the bump, the front wheel axle bar now exerts a negative moment on the top link. The opposing force is noted in Figure 15.

The top link continues to angularly accelerate until the moment applied by the front wheel axle bar is equal to the moment applied directly by the spring. The moment balance for this specific situation is shown in Equation (7).

$$\Sigma M = 0 = x_s F_2 - x_a F_a \quad (7)$$

At this instant, the top link ceases to accelerate. While this is another equilibrium point, it is unstable because the top link also has some amount of momentum. This momentum continues to carry the top link around the pivot at some angular speed.

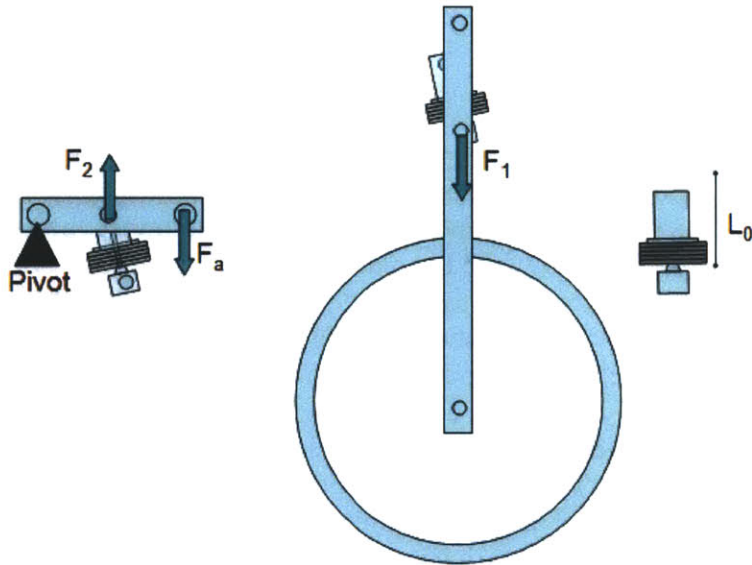


Figure 16: The Spring's Maximum Compression. The elements continue to move until the spring reaches its maximum compression.

The spring continues to be compressed, as seen on the far right of Figure 16, until the angular velocity of the top link slows to zero due to the angular deceleration caused by the imbalanced moments. At this point, the entire system has ceased to move. However, the forces have become imbalanced due to the additional compression of the spring.

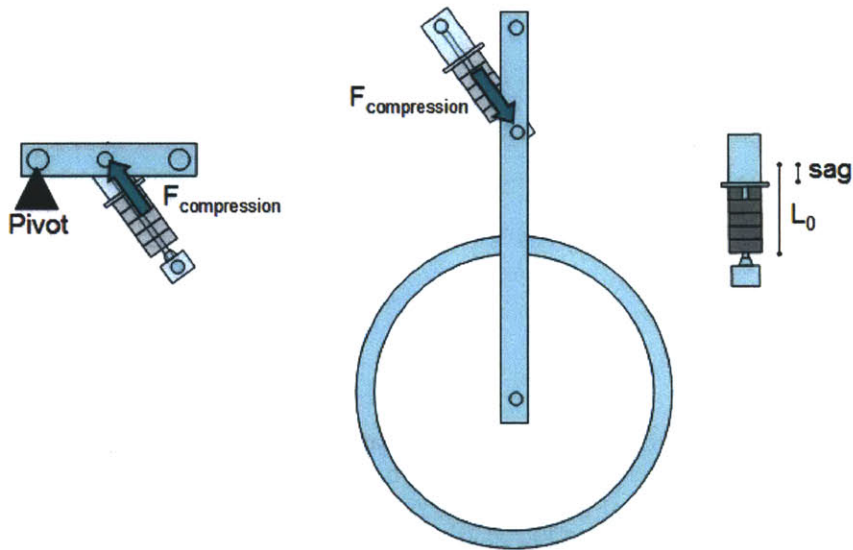


Figure 17: Returning To Neutral Position. The spring finally begins to decompress.

The spring begins to decompress as the top link and the front wheel axle experience accelerations due to the force imbalance. Both the top link and the front wheel axle begin to move back toward their original positions, shown in Figure 17. Ultimately, they come to rest, returning to the same configuration in which they were originally found before the bicycle drove over the bump.

This entire process of going over a bump happens in a fraction of a second. But by understanding these force balances, it is possible to determine what variables will have an effect on the system's performance.

### 4.3 Parameters That Affect Performance

The suspension system's functionality is based on the system's ability to absorb the force of a bump through the motion of its parts. The stiffness of the spring determines the amount the system must travel to exert a given force, while the placement of the mount within the suspension system's structure determines how the spring's force is applied to work against the motion caused by the bump. Three variables, shown in Figure 18, affect the suspension system's performance. The diameter  $d$  of the tire rubber donut will affect the force each individual tire rubber donut can exert by changing its original cross-sectional area. The length  $L$  of the stack itself should alter the maximum travel of the system because the engineering strain will remain constant. The distance  $h$  between the spring mount's position on the top link and the pivot between the top link and the front wheel axle bar will alter the force balance. This distance changes the angle at which the force of the spring is applied to the front wheel axle bar and to the top link. The percentage of the spring's force that operates perpendicular to the top link is related to the size of this angle. This distance  $h$  also affects the percentage of the spring force that is parallel to the front wheel axle.

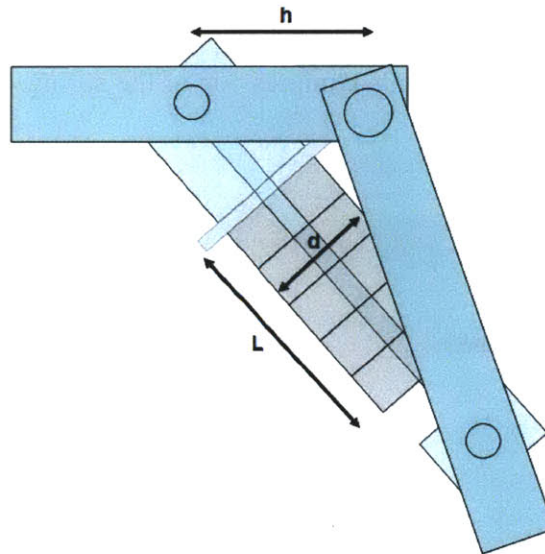


Figure 18: Experimental Variables of Interest. The diagram shows the top link and the front wheel axle bar. Not shown are the handlebars, which would appear in the top left of the diagram, and the wheel, which would appear in the bottom right. By varying the diameter  $d$  of the tire rubber donuts, the length of the tire rubber donut stack  $L$ , and the distance between the spring mount's position on the top link and the pivot between the top link and the front wheel axle bar  $h$ , the optimal configuration for the spring can be found.

#### 4.3.1 The Importance of Spring Stiffness

The spring will ideally act as has been described in the Section 4.2. The stiffness—given by the Young's Modulus—of the spring will determine exactly how the suspension system functions. There are two limiting cases to consider when dealing with spring stiffness. It will aid in understanding the cases to refer back to Figure 10.



### Case 1: Rigid Spring Material

The force of the front wheel striking the bump causes the front axle to rise. When the spring is made of a completely rigid material, the entire fork will rise as well. Therefore, all the force due to the vertical acceleration of the fork going over the bump is transmitted to the rickshaw driver's body.

### Case 2: Infinitely Compressible Spring Material

The force of the front wheel striking the bump causes the front axle to rise. The top links pivot up, much like in Figure 10b, as the spring compresses. The handlebars are able to remain in the same exact position.

Sadly, if the spring was actually infinitely compressible – or if a real world spring is simply not stiff enough—the spring would become coil bound, causing the suspension system to *bottom out*. Bottoming out means the system has hit some sort of final metal-to-metal contact after which point it behaves as though there is a rigid bar (Case 1) in place of the spring material. For example, the beta-prototype would bottom out if the tire rubber donuts compressed so much that the rod inside the tire rubber donuts was able to hit the mount's top link attachment rod. Equally problematic for the longevity of the suspension system would be any additional force exerted on the spring after it has become coil bound. Additional force on a coil bound spring will often lead to the permanent deformation of the metal. Even elastic materials, such a rubber, will eventually reach a tensile limit and begin to permanently deform.

### 4.3.2 The Mount's Geometry

The location of the mount determines at what angle the spring's force acts. For this experiment, the mount will be attached at three different points along the top link, while the attachment point to the front wheel axle bar remains constant. Each of these positions will enable the spring's force to act at a different angle to both the top link and the front wheel axle bar. The geometry associated with these three positions can be seen in Figure 19.

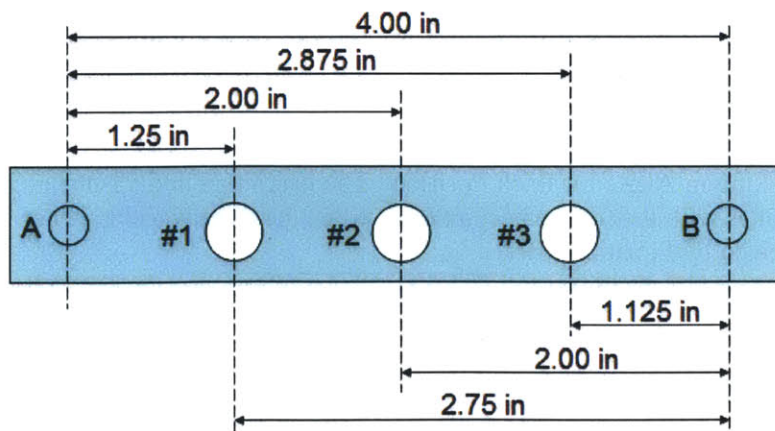


Figure 19: Dimensions of the Top Link. The three positions to which the mount can be attached are numbered: Position 1, Position 2, and Position 3. Pivot A is the pivot point between the handlebar bar and the top link. Pivot B is the pivot between the top link and the front wheel axle bar. The distances shown above the top link are the lengths of the moment arm for a given pivot. The distances shown below the top link are length  $h$  for each position.

When the spring is mounted in a position, the angle it can make with the front wheel bar is limited. In fact, the largest angle the spring will make with the front wheel axle occurs when the top link is perpendicular to the front wheel axle. By using Equation (8), the maximum angle  $\beta$ , shown in Figure 20, can be calculated.

$$\tan \beta = \frac{h}{6.5} \quad (8)$$

The distance  $h$  is based on the position to which the mount is attached and can be found in Figure 19.

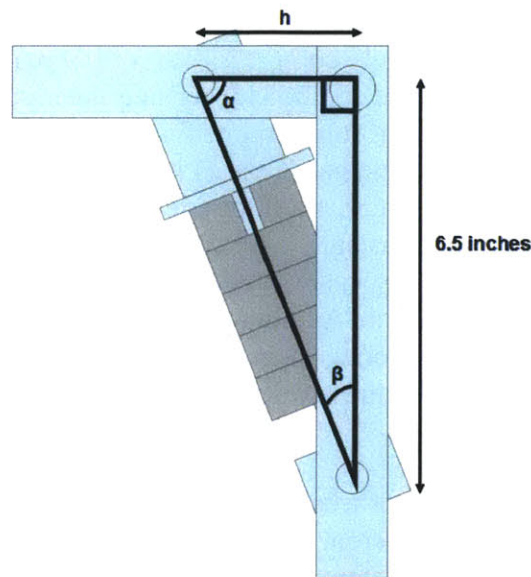


Figure 20: Defining  $\alpha$  and  $\beta$ . A greater percentage of the spring's force is applied in the direction of the front wheel axle when  $\beta$  is smaller. A greater percentage of the spring's force is applied perpendicular to the top link when  $\alpha$  approaches  $90^\circ$ .

This calculation is useful because a smaller angle will allow a greater percentage of the spring force to be exerted along the length of the front wheel axle bar. The maximum angle calculated for each position is shown in Table 1.

Table 1: The Maximum Angle for Each Position. The maximum angle is the angle  $\beta$  that the spring mount makes with the front wheel axle bar when the front wheel axle bar is perpendicular to the top link, given by Equation (8).

Position	Maximum Angle $\beta$
1	$22.9^\circ$
2	$17.1^\circ$
3	$9.8^\circ$

When the spring is mounted at Position 3, it is very close to being parallel with the front wheel axle bar. Therefore, a greater percentage of the spring force is exerted along the length of the front wheel axle bar. This force will limit the acceleration of the front wheel axle in the vertical

direction. Positions 1 and 2 have similarly sized maximum angles and can be expected to perform similarly in practice.

Even more important than the force applied along the front wheel axle bar is the force applied perpendicular to the top link. The entire suspension system works based on the amount of travel the system undergoes when externally forced. The travel, as previously mentioned, can be measured by how much the spring compresses. It can also be thought of in terms of the amount the top link pivots. The top link will pivot when the moments applied to the link are not balanced. A stronger directly applied spring force will cause a greater angular acceleration, and therefore a larger angle will be circumscribed.

The size of the moment created by a specific position is based on two factors: the length of the moment arm and the size of the angle  $\alpha$  made with the top link. First, for a set force, a larger moment arm will allow the force to apply a greater moment, as seen in Equation (6c). Second, when the spring mount forms a  $90^\circ$  angle with the top link, all of the spring's force would be used to generate a moment. When the spring mount is at something less than  $90$  degrees, only a portion of the spring's force is being used to generate a moment.

The placement of Position 3 allows the spring to create a large moment in two ways. First, Position 3 has the longest moment arm of the available options. Second, when the spring is mounted in Position 3, it is closer to being perpendicular to the top link than it is at the other positions with shorter moment arms. Therefore, Position 3 has an advantage over the other potential positions that have shorter moment arms and make smaller angles with the top link.

## **5 Apparatus and Procedure**

Having recognized tire rubber as a potentially useful material for the suspension system's spring, it is necessary to discover exactly what configuration will best cushion the rickshaw driver from the rough roads. The quantity of interest is the force felt by the rickshaw driver compared to a given force applied to the front wheel by the road. This force on the driver is directly related to the acceleration of the handlebars. Similarly, the force applied to the front wheel is directly related to the acceleration of the wheel axle. Therefore, by comparing the acceleration of the front wheel axle to the acceleration of the handlebars, the effect of having a certain spring configuration can be obtained. The optimal suspension system configuration will be a combination of the mount's attachment geometry, the length of the tire rubber donut stack, and the diameter of the tire rubber donuts diagramed in Figure 18. The optimal combination of these three variables will lead to the smallest acceleration of the handlebars for a given acceleration of the front wheel axle.

In order to collect the experimental data, one variable of interest was altered while the other two were held constant. Four trials for each configuration were run. While nearly infinite alterations are possible, only a finite number were selected to be tested. The specific values for the tire rubber donuts' diameter can be found in Table 2. The length of the tire rubber donut stack could easily be varied to almost any length by carefully choosing how many tire rubber donuts would

be placed in the mount\*. The attachment point for the mount was varied between three positions in accordance with Figure 19.

Table 2: Experimental Variable Options. This table lists the array of diameters used for the tests. The length, position, and diameter were used in any combination. The diameter's measurement is the measurement of the inner diameter of the hole saw used to make the tire rubber donuts and is not necessarily the exact size of the donuts created due to the tire rubber's tendency to elastically deform while being cut into donuts.

Diameter $d$
1.5 inches
0.870 inches
0.730 inches

### 5.1 Experimental Set-Up

To find the optimal combination of mount position and tire rubber donut diameter and stack length, the suspension fork was mounted to the front of a modern bicycle, shown in Figure 21. The front wheel of the bicycle was replaced with a rickshaw tire. Rickshaw tires look very similar to mountain bike tires, but have larger radii and more spokes than standard bicycle tires. The rickshaw tire was then pumped up to 60 psi, the maximum air pressure suggested by the manufacturer†, to simulate how the rickshaw drivers' generally fill their tires.

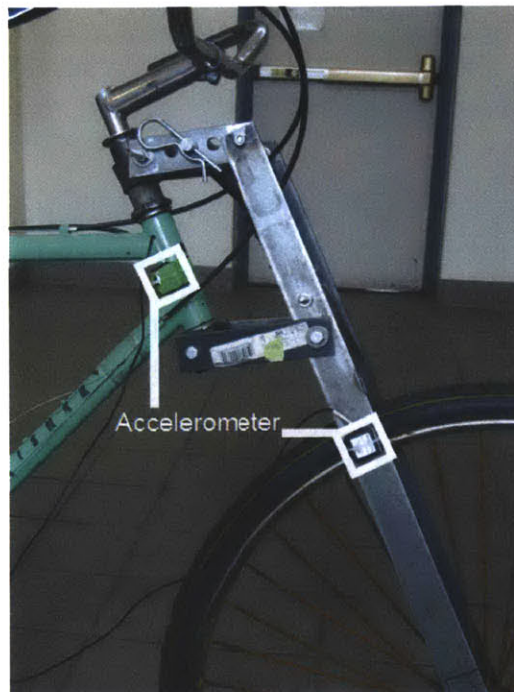


Figure 21: Experimental Set-Up. The two accelerometers are boxed. One is attached to the frame—which will have the same acceleration as the handlebars because they are rigidly connected. The other is attached to the front wheel axle bar. When the bicycle is driven in a straight line, the accelerometers are in parallel.

\* The length of each tire rubber donut varied because of variations in the tire's sidewall thickness.

† The maximum air pressure was embossed on the outside of the tire during the manufacturing process.

Two accelerometers\* were then attached to the suspension system, as shown in Figure 21. One was attached to the right front wheel axle bar, about 13 inches above the wheel axle. The other was attached to the bicycle head tube such that it would be parallel to the other accelerometer when the bicycle was driving in a straight line.

## 5.2 Testing

Having been equipped with two accelerometers, the bicycle with the suspension fork was driven around MIT's campus, while a Vernier LabQuest recorded the time-based data. For a given combination of donut stack height, donut diameter, and mount attachments, four trials were run. For each trial, the LabQuest took 200 samples/second for 60 seconds. Before each trial began, the LabQuest was reset and the bicycle was held such that the two accelerometers were parallel to one another when their readings were zeroed.

Amherst Alley, colloquially referred to as Dorm Row and shown in Figure 22, was selected as the road on which to conduct the tests because it provided a variety of different sized bumps and holes to ride over. The bicycle was driven at roughly the same speed for all trials. Each trial captured a slightly different portion of Amherst Alley between McCormick Hall and New House.



Figure 22: Amherst Alley. The experimental data was collected by driving down Amherst Alley between McCormick Hall (W4) and New House (W70). Burton-Connor (W51) is also shown. The path used during the experiments is marked with a red line.

## 5.3 Analysis Tools

The best way to quantify a specific configuration's effectiveness is to characterize the suspension system's frequency response. The response function for data that was recorded as a function of time can be found by using a fast Fourier transform (FFT). FFT takes functions of the time domain and converts them to functions of the frequency domain.

Each of the four trials for a given configuration was downloaded from the LabQuest and opened as a LoggerPro file. LoggerPro graphed the accelerations as functions of time. This time

\* The accelerometers used were 25-g accelerometers from Vernier Software and Technology, Inc.

domain data was then exported to a text (.csv) file, to prepare it to be read by MathCad, an engineering calculations software package.

Using a MathCad program based on Ian Hunter's *System Identification Via FFT*,\* the frequency response function was estimated for each trial. First, the program imported the time domain data text file. After each column of the imported file was denoted as the time, the input, and the output, the program ran an FFT to find the input-power spectrum, shown in Figure 23. Power, shown on the left axis, is the square of the amplitude of the FFT. The amplitude is related to the percentage of the signal that appears at a given frequency. So, it can be said that the power is directly related to how many measurements were made at a given frequency.

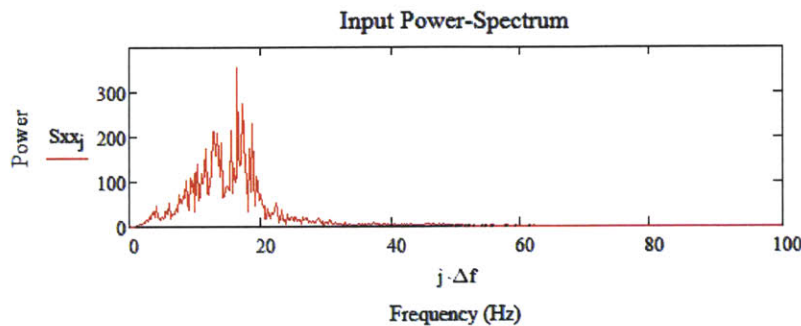


Figure 23: Input Power-Spectrum. This is the Input Power Spectrum for one trial where the tire rubber donuts were 0.870 inches in diameter and were stacked such that their uncompressed height was 3.5 inches. The mount was attached at Position 1, the position in the top link closest to the handlebars.

The physical meaning of the frequency is very important. The frequency is a measure of how rapidly the suspension system felt forces from the road. A large bump, like a speed bump, would exert a force for a longer period of time. Because the period of time and frequency are inverse functions of one another, as demonstrated in Equation 9, this means that a speed bump has a low frequency.

$$T = \frac{1}{f}, \quad (9)$$

where  $T$  is period and  $f$  is frequency.

The duration of a bump is not only related to the size of the bump, but also to the speed with which the bicycle rides over the bump. Because of the heavy inner city traffic, a single gear ratio, and difficult terrain, one might estimate a rickshaw's average speed as twice or thrice that of a person's regular walk. For this experiment, the bicycle was ridden along Amherst Alley at approximately that same pace for each trial.

Once the Input Power-Spectrum was graphed, the program calculated the input output cross-spectrum by taking the FFT of the cross product of the input and output data. The frequency response function was then calculated by dividing the input output cross-spectrum by the input power-spectrum. The frequency response function was then graphed in Figure 24 as a Bode

\* See Appendix D for the complete MathCad code.

Plot, showing both magnitude and phase. The Bode Phase Plot is included for completeness, but will not have any effect on the rickshaw driver's comfort. Therefore, it is the Bode Magnitude Plot that matters most for these experiments and will hereafter be referred to as the Bode Plot.

The Bode Plot shows Gain graphed as a function of frequency. This gain can be thought of as the output divided by the input for a given frequency. So, if the spring was replaced with a rigid rod, as discussed in 3.3, the Gain should be 1. The suspension system is providing some cushion at all gain values that are less than 1. Obviously, a gain of 0.9 is really doing very little to help cushion the rickshaw drivers' bodies from the rough road conditions.

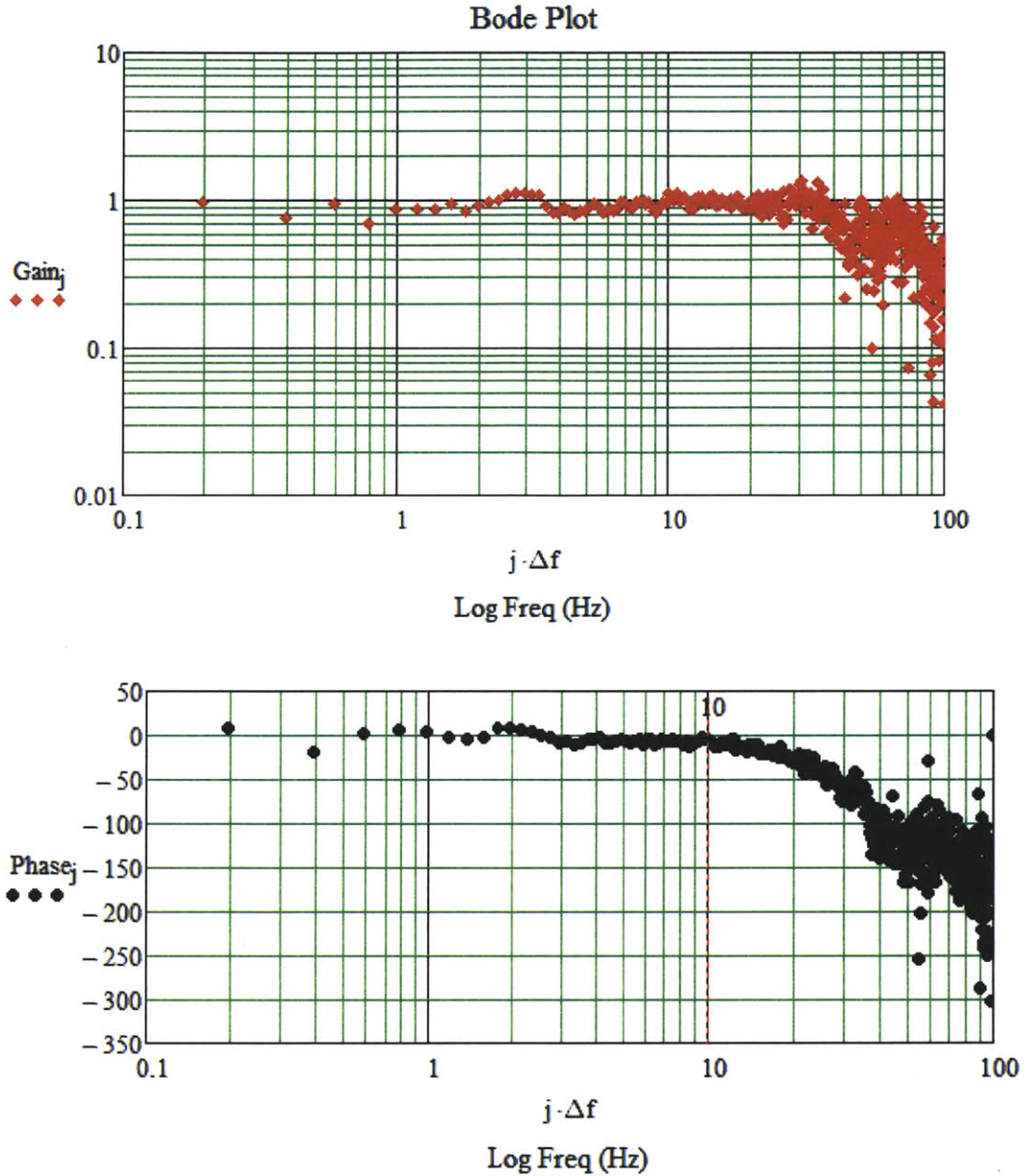


Figure 24: Bode Plot. The top half of the figure is the Bode Magnitude Plot. The lower half of the figure is the Bode Phase Plot, which provides no relevant information in this context. This is the Bode Plot for one trial where the tire rubber donuts were 0.870 inches in diameter and were stacked such that their uncompressed height was 3.5 inches. The mount was attached at Position 1, the position in the top link closest to the handlebars. Notice that both axes on the magnitude plot are a log scale, while the phase plot uses a linear scale for the phase and a log scale for the frequency.

For each trial, the resulting frequency and gain were exported to an Excel file. In the Excel file, the average gain for all trials of each specific configuration was computed as a function of frequency. This average gain was then graphed against the frequency to give an average Bode Plot for each configuration, an example of which can be seen in Figure 25.



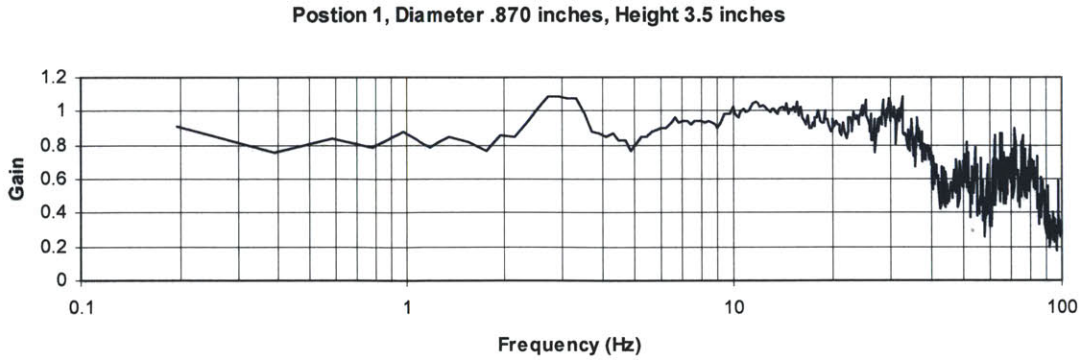


Figure 25: Bode Plot with Average Gain. This Bode Plot is the average of four trials where the tire rubber donuts were 0.870 inches in diameter and were stacked such that their uncompressed height was 3.5 inches. The mount was attached at Position 1, the position in the top link closest to the handlebars. Notice that only the frequency axis is a log scale. The gain was left as a linear scale in order to allow the reader to better see the variations in gain.

#### 5.4 Figure of Merit $\phi$

In order to quantitatively compare the performance of one configuration to another, a figure of merit must be defined. The figure of merit  $\phi$  will be the average of the gain for a particular frequency range. The gain used to calculate  $\phi$  will be the gain found by averaging the values of the four trials together. Therefore,  $\phi$  will be best described as the average of the average gain. The frequency range used to calculate  $\phi$ , which will be further defined in Section 6.1, should be the frequency range that best represents the frequencies experienced by rickshaw drivers as they drive along the rough Indian roads.

This calculation will always be stated with a 95% confidence interval. The 95% confidence interval is calculated using Equation (9).

$$\phi = \frac{1.96 * \kappa}{\sqrt{n}}, \tag{9}$$

where  $\phi$  is the uncertainty,  $\kappa$  is the standard deviation of the gain, and  $n$  is the number of points taken within the frequency range.

If the value of  $\phi \pm \phi$  for a specific configuration overlaps with  $\phi \pm \phi$  for another configuration, the performance of those two configurations is indistinguishable.

### 6 Testing Results and Discussion

Twelve different configurations were tested in order to deduce what the best possible system would be for the suspension system of the rickshaw. Four trials were run for each configuration, so that several frequency response functions could be averaged together to decrease noise in the results.

### 6.1 Finding India at MIT

It is not reasonable to expect a low cost suspension system to protect the rickshaw driver from every size abnormality on the roads of India. In fact, it is unnecessary to defend the driver's body against anything larger than a speed bump, which—when driven over slowly—amounts to about 1 Hz or something as small as very fine gravel, which could be as much as 100 Hz. Therefore, it is necessary to determine at what frequency range the suspension system will provide the greatest benefit to the driver.

By driving over a portion of road that would be representative of India and calculating the Input Power-Spectrum, it is possible to determine what frequencies appear most often. A portion of Amherst Alley, in front of the MIT dorm Burton-Connor, fits the bill for a rough Indian road. A side-by-side comparison of the two can be seen in Figure 26.



Figure 26: Indian Road Versus MIT Road. (a) This photo shows a rickshaw riding down one of the main roads in Guwahati, the capital of the Indian state of Assam. (b) This is a photo of Amherst Alley in front of the MIT dorm Burton-Connor. The road conditions are quite similar!

The data was taken for 10 seconds at a sampling rate of 200 samples/second. The bicycle with the suspension system was driven a very short distance on the flat, generally smooth pavement to get up to speed before it was ridden over the particular portion of interest. Five trials were conducted, but the data for the final three had to be discarded because of an obvious misalignment of one of the accelerometers. The Input Power-Spectrum shown in Figure 27 was generated using this data.

## On the Road In Front of Burton-Conner

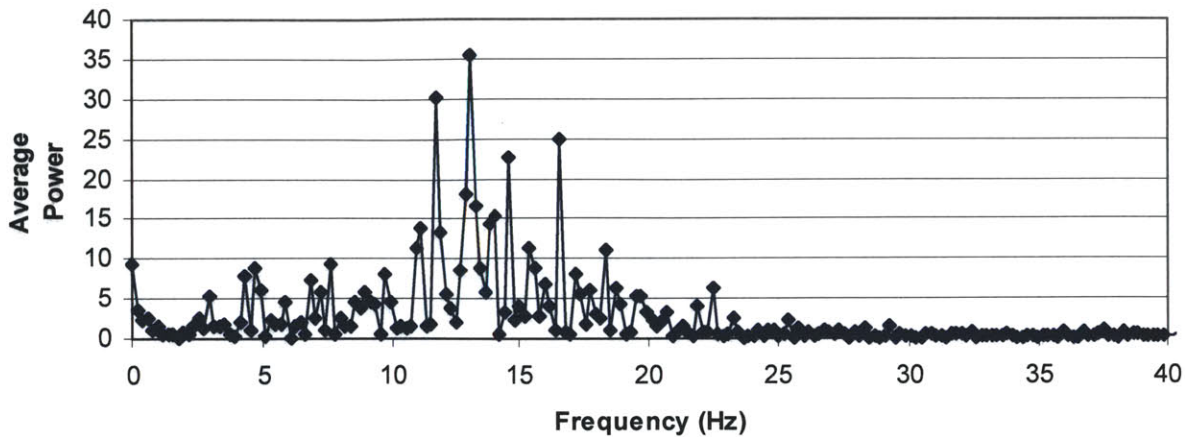


Figure 27: Input Power-Spectrum Used To Determine Frequency of Interest. The Input Power-Spectrum's power values, graphed here, were averaged over two trials.

According to the Input Power-Spectrum, the rickshaw drivers would be driving on roads at a speed such that the frequency of greatest concern is 10-20 Hz. Therefore, the effectiveness of the configurations for the rickshaw suspension system will be evaluated for that region.

### 6.2 Finding Appropriate Configuration

By comparing the average Bode Plots\* for each configuration, several interesting discoveries were made with regards to what experimental variable had the greatest impact on the operation of the suspension system.

While holding the diameter of the tire rubber donuts at 0.870 inches and using the mount at Position 2, the number of tire rubber donuts held in the mount was varied. The resulting Bode Plot is shown in Figure 28. Because strain is constant, the amount that the spring compresses increases as the length of the stack increases, for a given force. Somewhat unexpectedly, Figure 28 shows that length had no effect on the system's response.

For this experiment, the rest of the geometry—including the length of the one inch tubing—was held constant while the tire rubber spring's length was varied, which meant that a change in the length of the tire rubber donut stack also changed the angles  $\alpha$  and  $\beta$ , defined in Figure 20. The variations in angles  $\alpha$  and  $\beta$  counteracted any gains that would have been made by changing the length of the stack.

For a shorter stack, angle  $\alpha$  would be significantly larger, while  $\beta$  would remain approximately the same. This larger angle  $\alpha$  would allow a greater portion of the spring's force to act on the top link. In order to balance the moments on the top link, as shown in Figure 15, the system would need to compress further before the force applied by the spring to the front wheel axle bar would be strong enough to counteract this force directly applied by the spring to the top link.

\* Bode Plots of additional configurations can be found in Appendix E.

In summary, there is no discernable difference between stacks of differing length because the variations in the angles  $\alpha$  and  $\beta$  counteract the increase in the actual change in length. The length of the tire rubber donut stack has no noticeable effect on the Gain of the suspension system.

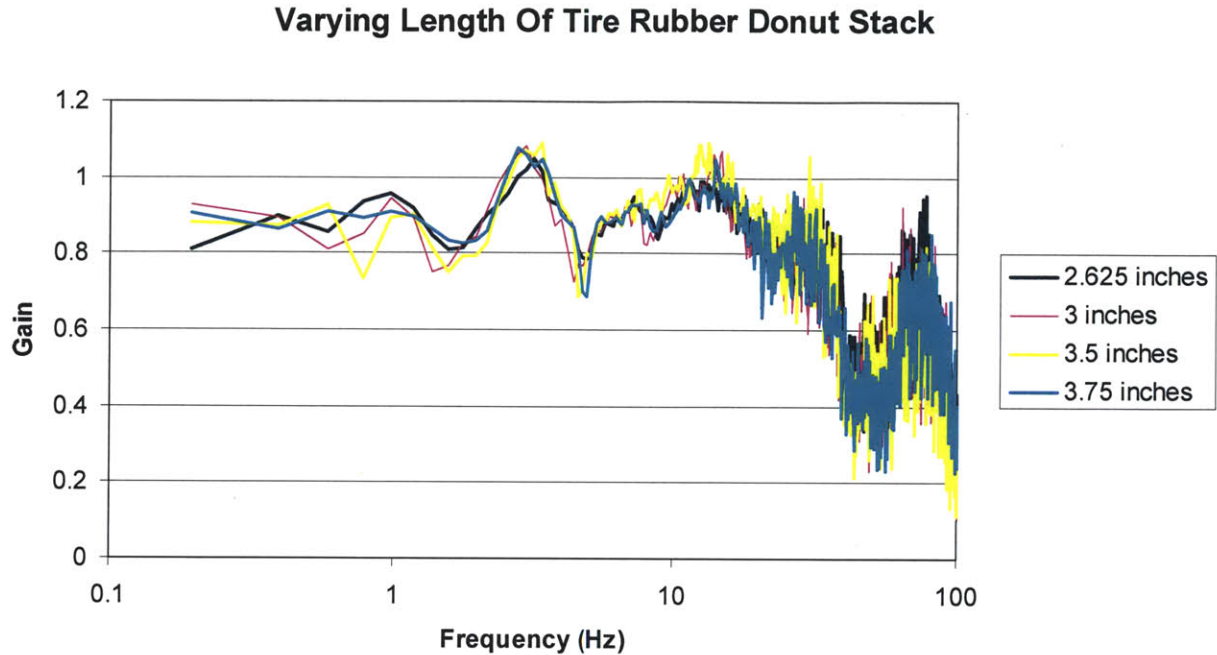


Figure 28: Varying Length of Tire Rubber Donut Stack (Log Frequency). The graph shows four configurations, each using a different length stack of uncompressed tire rubber donuts. For these trials, the tire rubber donuts had a diameter of 0.870 inches and were mounted in Position 2.

Being mindful that a log frequency plot makes it difficult to discern if there is a small but significant perturbation at the frequency band of interest, it is necessary to look also at a linear plot of the frequency band that most affects rickshaw drivers. Figure 29 zooms in on the 10-20 Hz region to allow for a better view of this important frequency band. Removing all intermediate lengths, there is still no difference on how the system reacts to a given frequency based on the length of the tire rubber donut stack.

### Varying Length of Tire Rubber Donut Stack

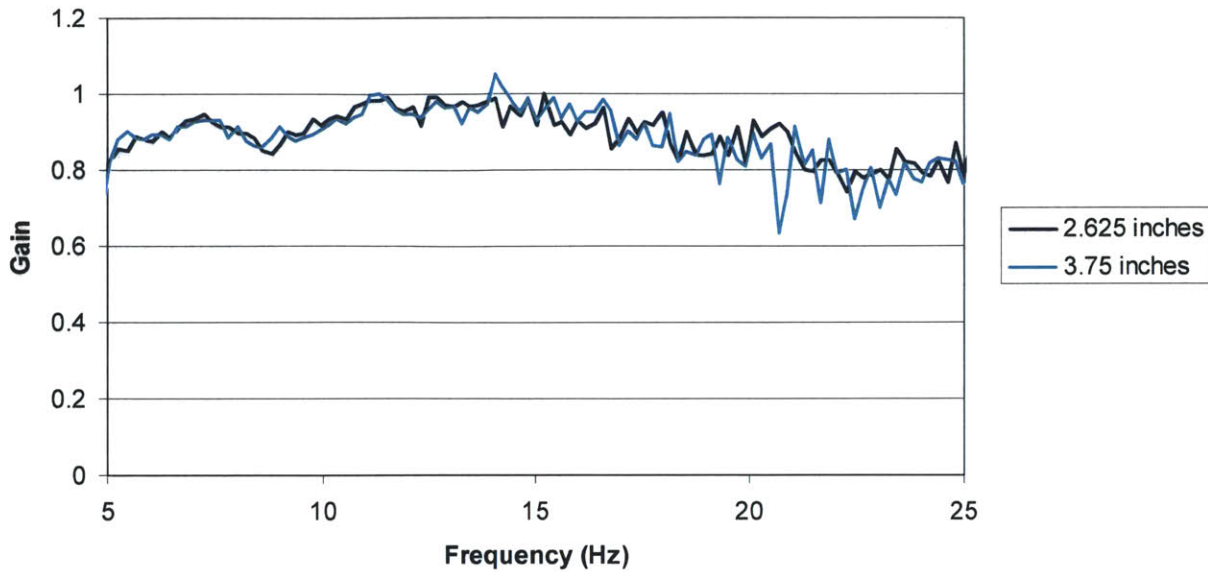


Figure 29: Varying Length of Tire Rubber Donut Stack (Linear Frequency). The graph shows two configurations, each using a different length stack of uncompressed tire rubber donuts. For these trials, the tire rubber donuts had a diameter of 0.870 inches and were mounted in Position 2. The frequency band that best represents the frequencies experienced by Indian rickshaw drivers is 10-20 Hz.

Even when using the figure of merit  $\phi$  for each of these configurations, shown in Table 3, there is still no discernable trend based on length. In fact, the smallest stack length's  $\phi$  is actually completely held within the bounds of the largest stack length's  $\phi$ , much like Figure 29 suggests.

Table 3: Figure of Merit Varies With Length. For these configurations, the diameter of the tire rubber donuts was 0.870 inches and the mount was in Position 2. The length was varied by adding or removing tire rubber donuts. These lengths are the uncompressed lengths of the tire rubber donut stack.

Length (inches)	$\phi$
3.75	$0.93 \pm 0.02$
3.5	$0.97 \pm 0.02$
3	$0.93 \pm 0.02$
2.625	$0.93 \pm 0.01$

This being said, it is important to recall that too much compression will lead to bottoming out. This happened for several stacks of 0.730 inch diameter tire rubber donuts when Position 3 was used. The average Bode Plot from one such configuration can be seen in Figure 30. The amount of compression was such that the front of the suspension fork actually knocked against the bottom of the handlebars. When this occurred, the shock to the handlebars caused them to accelerate *more* than the front wheel axle. Bottoming out is extremely counterproductive, as it makes the system amplify the force of the bump, rather than decrease its impact on the driver.

This amplification is indicated on the Bode Plot in Figure 30 by gain values that are greater than 1. The system's  $\phi$  while bottoming out is  $1.05 \pm 0.02$ , which stays above a gain of 1.

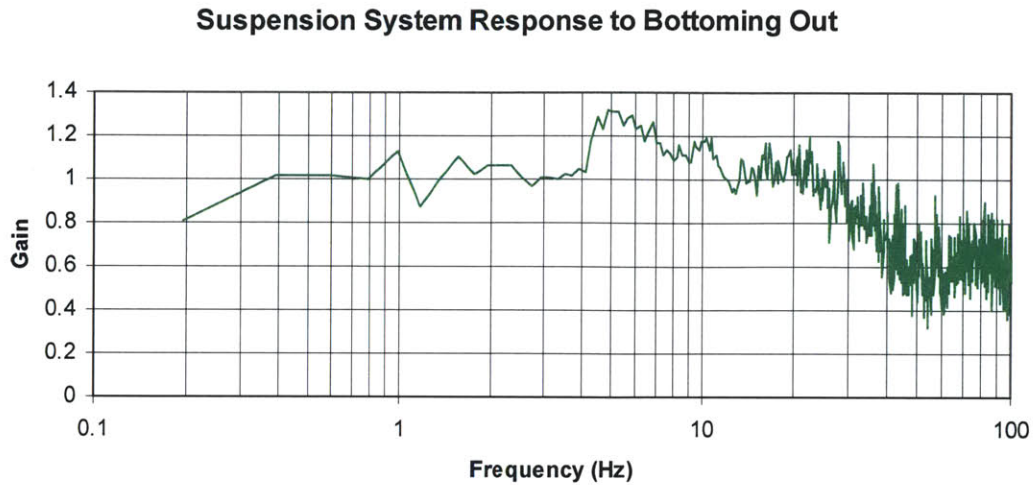


Figure 30: The Suspension System's Response to Bottoming Out. The suspension system is amplifying the force of the bump at all gain values greater than 1. For this experiment, the mount was attached at Position 3 with a 3.5 inch tall stack of 0.730 inch diameter tire rubber donuts. The suspension system bottomed out often during all four 60 second trials.

Measuring the effect of the diameter of the tire rubber donuts on the effectiveness of the suspension system was made possible by holding the position and the tire rubber stack length constant. Somewhat unexpectedly, Figure 31 shows that there appears to be no relationship between the diameter of the tire rubber donuts and system's Gain. In fact, for Position 2 with a tire rubber stack of 3.5 inches, the system response at 10 Hz is largest for a diameter of 0.870 inches but at 20 Hz is largest for a diameter of 1.5 inches. Even the smallest diameter (0.730 inches) causes the largest system response from 17-19 Hz.

### Varying Diameters at Position 2

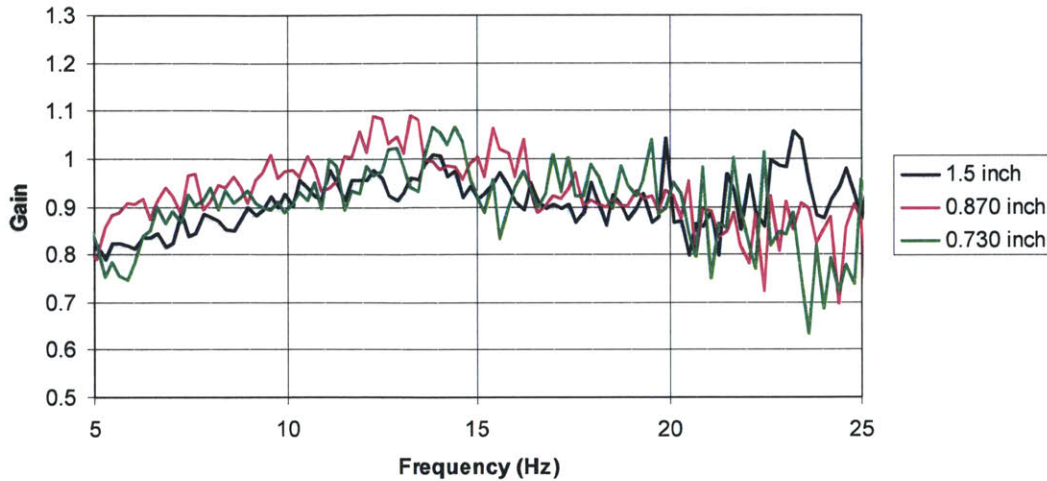


Figure 31: Varying Diameters. For these three configurations, the mount has attached at Position 2 and the tire rubber donut stack was 3.5 inches tall. Varying the diameter makes no discernable difference in the system response because smaller tire rubber donuts are able to be compressed more than their larger counterparts.

The configuration's values for  $\phi$  showcase the same lack of a logical relationship. The  $\phi$  for the configuration with a diameter of 0.730 inches overlaps with both of the other configurations. However, the  $\phi$  for the configuration with a diameter of 0.870 inches is always larger than the  $\phi$  for the configuration with a larger diameter. Yet, there is no clear relationship between the system response and the tire rubber donuts' diameter.

Table 4: Figure of Merit Varies With Diameter. For these configurations, the tire rubber donut stack was 3.5 inches tall and the mount was in Position 2.

Diameter (inches)	$\Phi$
1.5	$0.93 \pm 0.01$
0.870	$0.97 \pm 0.02$
0.730	$0.95 \pm 0.01$

This comes as quite a shock since the compressive force of the spring is based on the cross-sectional area of the tire rubber donuts. Referring to the Equation (5), the compressive force depends on the Young's Modulus, the area, and the strain. Young's Modulus is an intrinsic property and, as such, is constant at a given frequency. Therefore, as area decreases, strain must increase. An increase in strain means an increase in the overall compression of the spring material. Strain varies with the size of the rubber because of the effects of friction between tire rubber donuts and the thread ply embedded in the tires.

As previously mentioned, the threaded ply is inextensible and is embedded in the tire in layers. The tire rubber surrounding the threads can only expand between the threads in a manner that would move them further apart. This motion is opposed by the threads in the layer above that are lying at a different angle to the first layer. (See Figure 8 for visualization.) In tire rubber

donuts of a smaller diameter, there are fewer threads and, therefore, less interference with the radial expansion required for compression to take place.

There is also some resistance to radial expansion because of the frictional forces at each interface. Since these tire rubber donuts do not have perfectly smooth faces, the radial expansion (due to compression) is slowed as some tire rubber donuts (due to a slightly different pattern of ply threads or slightly different thicknesses) do not expand as quickly as others. Because friction is a contact force, the more area that is in contact at the interface, the more likely the interfaces are to impede one another's progress. Therefore, tire rubber donuts with a smaller cross-sectional area will experience less friction at the interface.

Lastly, the attachment point of the mount to the top link was varied while the diameter and stack length of the tire rubber donuts were held constant. As Figure 32 illustrates, this had by far the largest impact on the system's response.

**Comparison of all three positions using 3.5 inches of 0.870 inch diameter rubber**

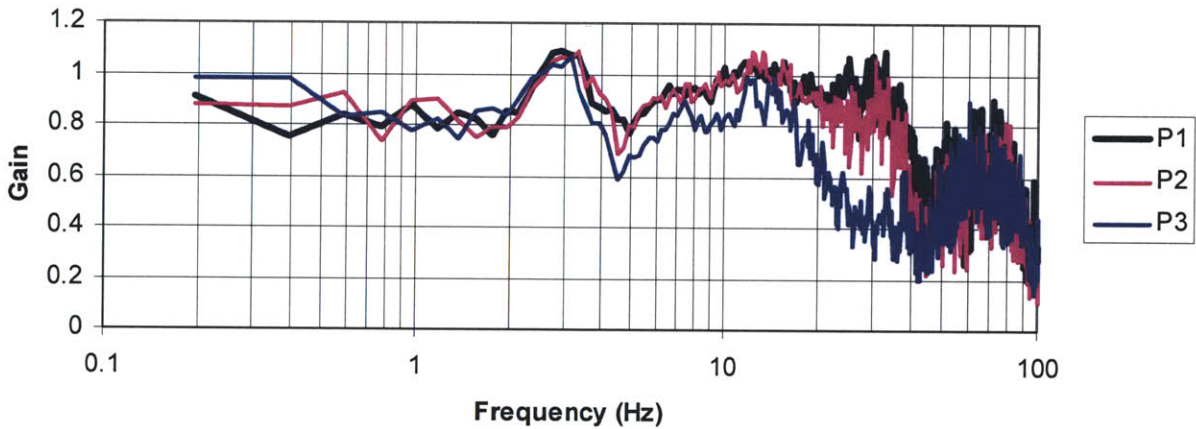


Figure 32: Varying Position. For these three configurations, tire rubber donuts with a diameter of 0.870 inches were placed in a stack measuring 3.5 inches, while the mount's attachment point to the top link was manipulated.

The suspension system performed best when the mount was placed in Position 3 with any variation of diameter and stack height that did not involve the system bottoming out. A plot of the linear frequency, shown in Figure 33, reveals that the mount attached to Position 3 gives a consistently better system response than either of the other two positions that were tested. In fact at 17.5 Hz, the gain for Position 3 is 0.65, while both Position 1 and 2 are well above 0.90.



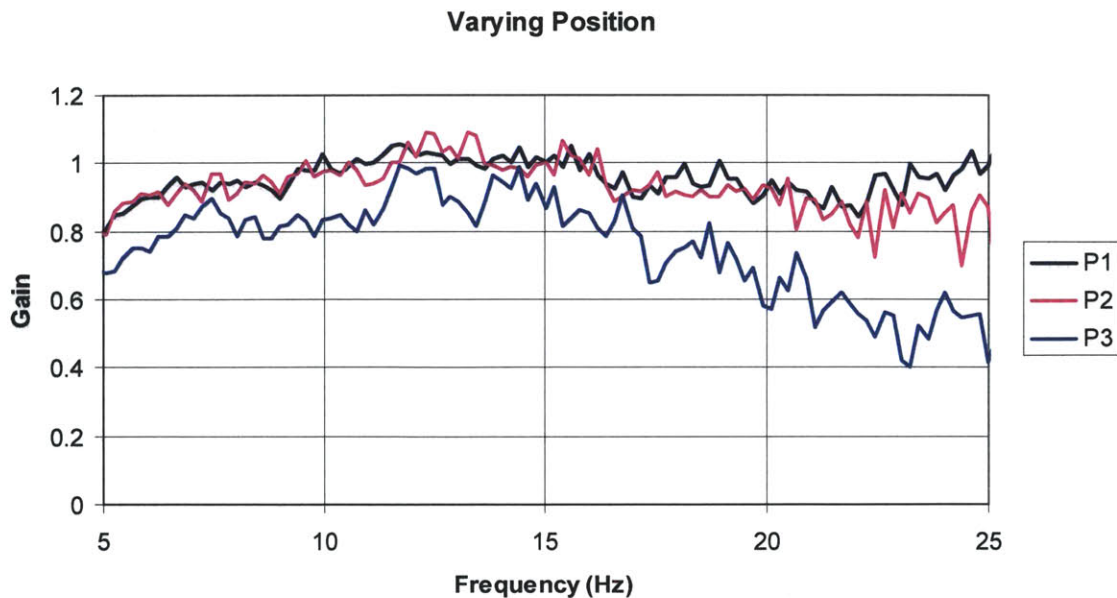


Figure 33: Varying Position. This graph is a closer look at frequency band that most affects the rickshaw drivers: 10-20 Hz. For these three configurations, tire rubber donuts with a diameter of 0.870 inches were placed in a stack measuring 3.5 inches.

Across the entire range of interest, Position 3 performs best, as shown in Table 5. While both Position 1 and 2 overlap significantly, Position 3 has a  $\phi$  of at least 0.10 better than the other positions and is the only position for which the value of  $\phi$  was significantly less than 1. This drastic difference in the system response over three mount attachment locations is due entirely to the angles the spring mount makes with the top link and the front wheel axle bar.

Table 5: Figure of Merit Varies With Position. For these configurations, tire rubber donuts with a diameter of 0.870 inches were placed in a stack that was 3.5 inches tall. Refer to Figure 19 for the complete geometry of the attachment points.

Position	$\Phi$
1	$0.99 \pm 0.01$
2	$0.97 \pm 0.02$
3	$0.83 \pm 0.03$

This discovery should come as no surprise given Position 3's geometry. Position 3 has the capability to provide a greater portion of the spring's compressive force along the front wheel axle and perpendicular to the top link, as detailed in Section 4.3.2.

To further magnify the gains made by Position 3's geometry, it would be wise to move the spring mount's attachment point to the top link as close to the pivot between the top link and the front wheel axle bar as possible. This position must not be so close to the connection point that it interferes with the structure's ability to pivot.

Another method for increasing the size of the angle  $\alpha$  while decreasing the size of the angle  $\beta$  would be to move the mount's attachment point to the front wheel axle bar. For these

experiments, the spring mount's attachment to the front wheel axle bar was constantly 6.5 inches below the pivot between the top link and the front wheel axle bar. However, if this distance was increased, it would positively impact the system's performance in the same way that increasing the moment arm of the spring's force on the top link does.

## **7 Conclusion**

Rickshaw drivers would benefit from having a front fork suspension system. A four bar linkage with a tire rubber spring would be an easy-to-build, adequate suspension system that looks very much like the current rickshaw forks. The tire rubber spring can be made out of donut shaped pieces of a used tire's sidewall that have been slid onto a rod and mounted into the fork structure. The mount should be placed such that the attachment point on the top link is as close to the connection between the top link and the front wheel axle bar as possible. This will ensure that full advantage is taken of the spring's compressive force.

The exact geometry of the tire rubber donuts does not matter for the response function of the suspension system. However, the geometry does have several effects. While the diameter of the tire rubber donuts makes little difference on how well the system responds to external forces, it does make a difference in how much material is used to create each suspension system. In order to conserve resources, a small diameter should be selected. The length of the stack of tire rubber donuts also has only a small effect on how well the suspension system performs. However, if the stack is too short, the suspension system runs the risk of bottoming out when the spring compresses. Therefore, it is recommended that the stack height be tested on an actual rickshaw to ensure that bottoming out will not occur regularly.

In conclusion, the entire system should be tested under real life conditions because a bicycle riding along Amherst Alley is not a perfect parallel to a rickshaw riding along a road in Guwahati, India. If the spring is properly mounted into the suspension system fork's structure, it will be able to provide some level of cushion for the rickshaw drivers at a low cost.

## Appendix A: Beta-prototype Dimensions

When the next version of the beta-prototype is fabricated at The Rickshaw Bank's factory in Guwahati, one inch tubing will be used for the majority of the suspension system's structure. Many of the pieces, their permanent dimensions established, could be welded into place. For example, both of the rods the spring mount attached to and pivoted around could be welded into place rather than have some sort of holes drilled and then pins attached to the ends.

In order to more easily experiment with the spring and the mount geometry, the beta-prototype suspension system structure was made such that it could be completely disassembled. Steel bars connected with threaded rod, removable round stock, and bolts were the primary components. Bearings were used at all of the joints. For added flexibility, these bearings were longer than the width of the top and bottom links which rode on the bearings. Washers, not shown in the diagrams in this appendix, were added to make up for the extra length not covered by the top and bottom links. These washers allowed the system to be fine-tuned to certain dimensions; however the washers added complexity that was not compensated for by the added flexibility.

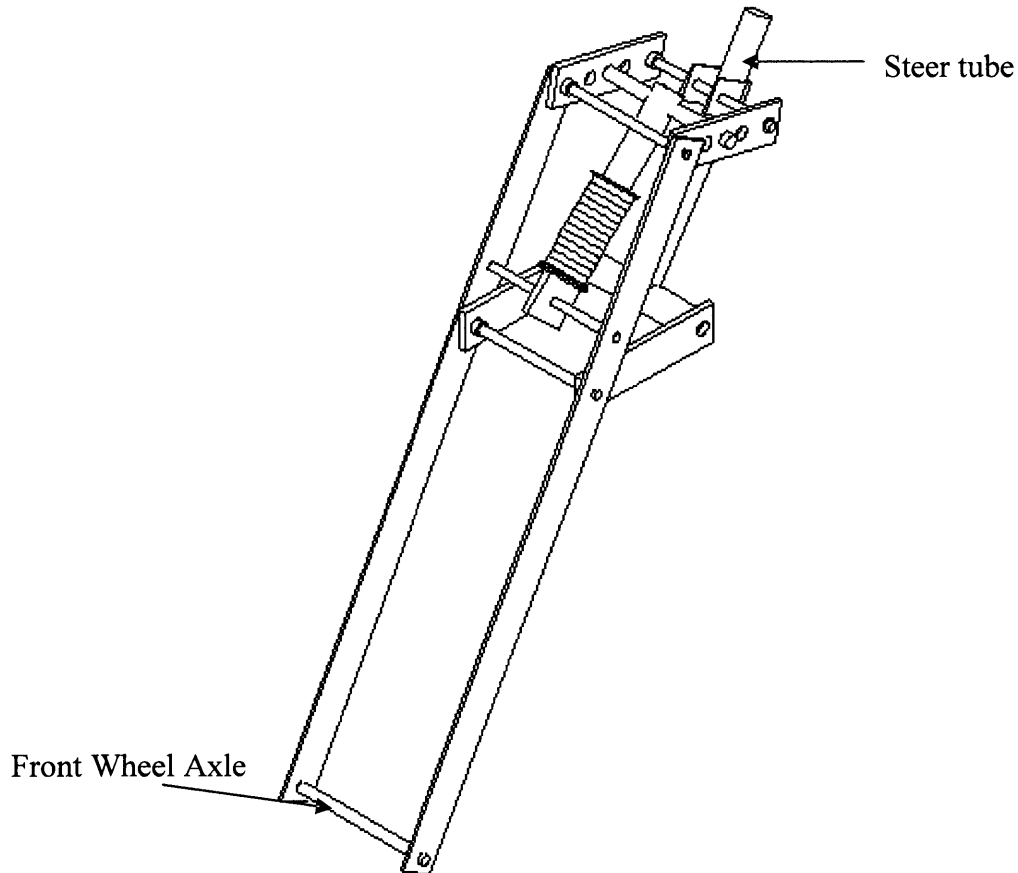
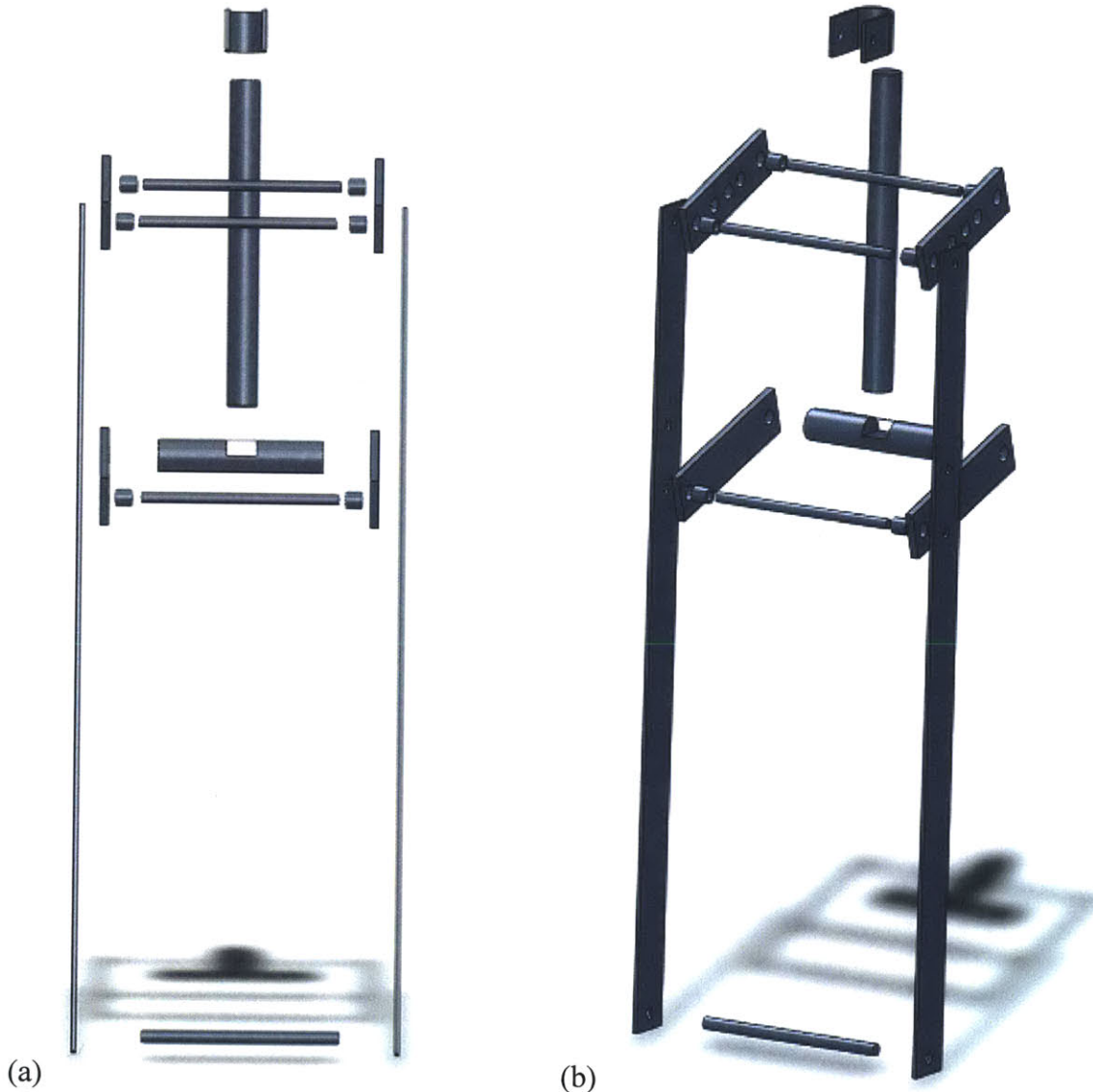


Figure A1: Isometric Drawing of Entire Suspension System. The front wheel axle is the bar in the lower left. The handlebars would attach to the steer tube, shown as the tube in the back and center of the structure.

## *Suspension System Structure*

Figure A2 gives an exploded view of the suspension system structure. The 3/8 inch bar shown at the bottom of the figure is a stand-in for the front wheel axle. The handlebars would be located on top of the steer tube—that is, the 0.9 inch tube in back and center of both drawings.



(a) (b)  
Figure A2: Exploded View of Suspension System Structure. (a) Front view, looking from wheel back towards the bicycle seat. (b) Angled View, where wheel would be in the bottom of the foreground.

The C shaped metal piece at the top of the exploded view is used to attach the top links to the steer tube. This C clamp, for lack of a better term, slides down over the steer tube and rests on the head tube, as shown in Figure A3. The locknut that normally holds only the steer tube in place with respect to the head tube also holds the C clamp in place in this design.

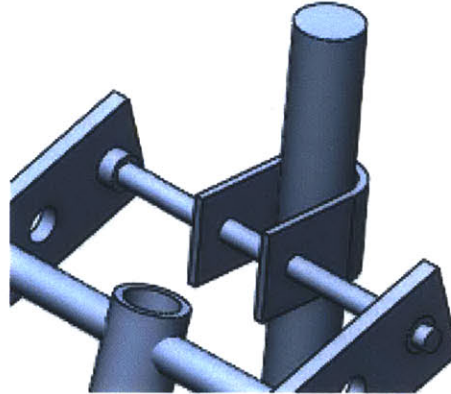


Figure A3: Assembled View of C Clamp. This diagram shows the C Clamp, steer tube, and top links as they would be assembled on the rickshaw's suspensions system.

The steer tube itself will need to be purchased. For the experimental prototype, the legs were sawed off of a bicycle fork, leaving only the crossbar and the steer tube behind. The crossbar of the bicycle fork was not removed, so that it could be used as the bottom pivot point on the handlebar bar. This will likely be the way that the suspension system is manufactured in Guwahati as bicycle forks are relatively cheap.



Figure A4: Exploded View of Right Top Link. The threaded rods on the right connect the top links together so that they will move in unison. Bearings were put at each pivot to enable the link to move with less friction. The front wheel axle bar, shown on the far left, was attached to the threaded rod and held in place with a nut (not shown). The threaded rod is wholly unnecessary when the system is made in Guwahati.

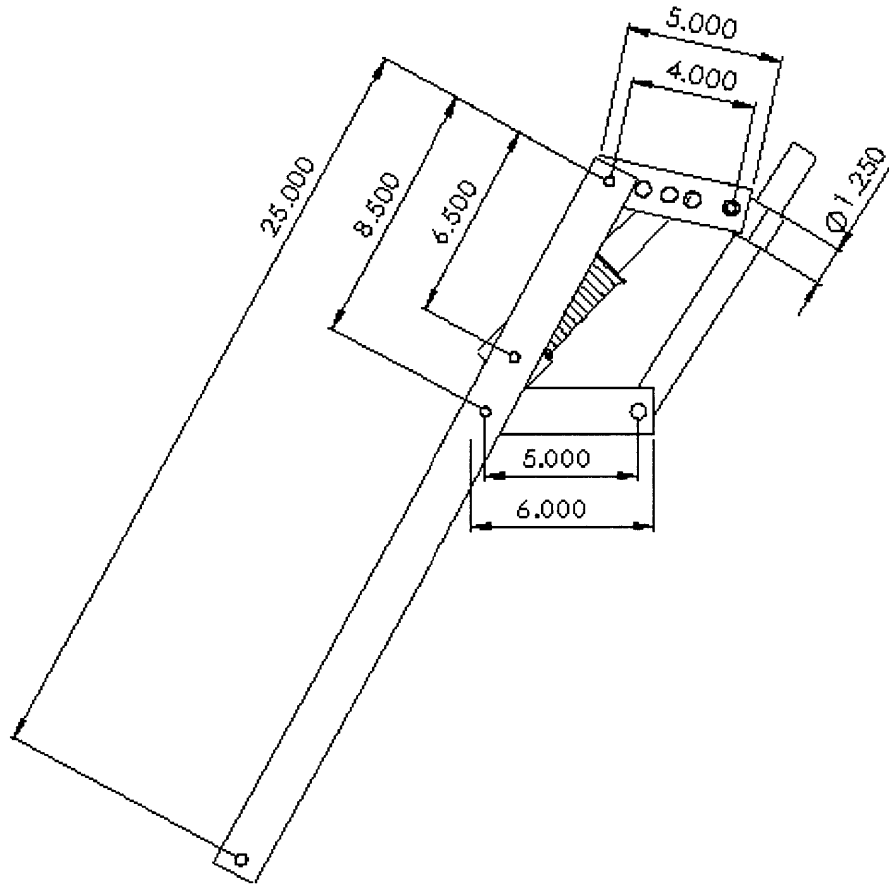


Figure A5: Lengths of Interest. These dimensions, shown in inches, will allow the rake of the new suspension fork to match the rake of the current forks.

The rake of a bicycle is measured as the distance between an imaginary line drawn straight through the center of the steer tube and the parallel line drawn through the axle. The rake determines how the bicycle steers. While most pleasure bicycles in the United States have a rake of only a few inches, the Indian rickshaws have about a five inch rake.

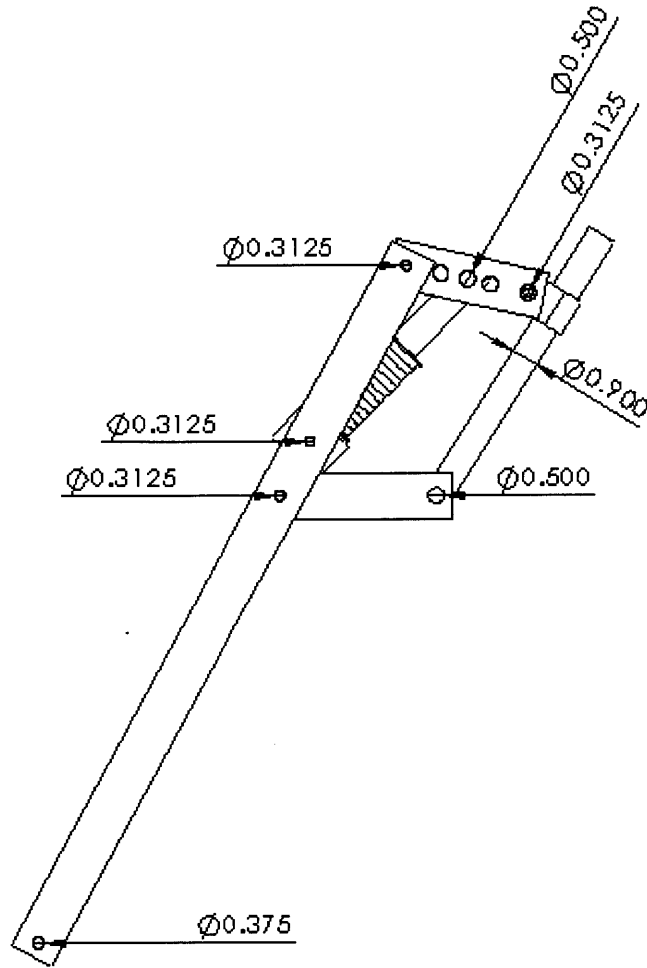


Figure A6: Diameters of Interest. These are the dimensions, shown in inches, used in the experimental version.

All of the dimensions shown in Figure A6 can vary in the Guwahati version based on the size of the rods available and the bearings used, except for the front wheel axle hole, which must be 0.375 inches to fit around the standard rickshaw tire wheel axle. If the other parts are welded together, this hole should be drilled and then slotted to allow the rickshaw driver to remove the fork.

### Spring Mount and Material

The spring mount diagrams shown below are all dimensioned with tire rubber donuts 1.5 inches in diameter and a  $\lambda_0$  of 0.25 inches, based on the thickness of the center of the tire sidewall. Not captured in these diagrams is the variation in the length of the tire rubber donuts. In actuality  $\lambda_0$  depends on the tire itself and the part of the sidewall from which the rubber donut is cut. These variations will affect the behavior of the system, as noted in Section 6.2.

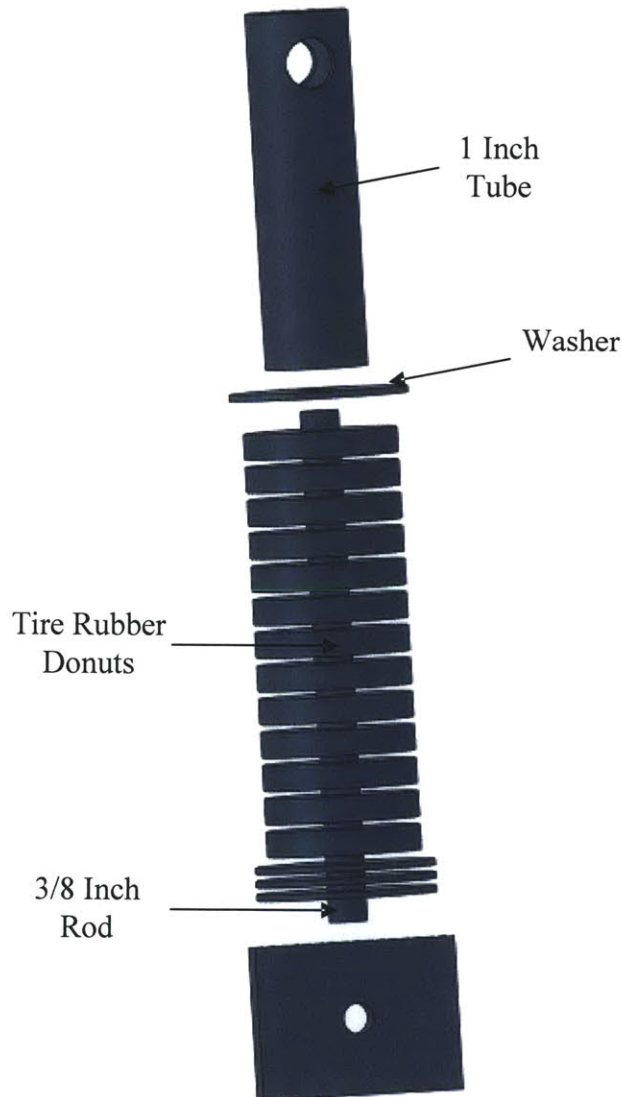


Figure A7: Exploded View of Spring and Spring Mount. This mount will change very little in between the experimental prototype and suspension systems built in Guwahati. The welding and minor drilling are completely within reach of the limited tooling available at The Rickshaw Bank's factory.



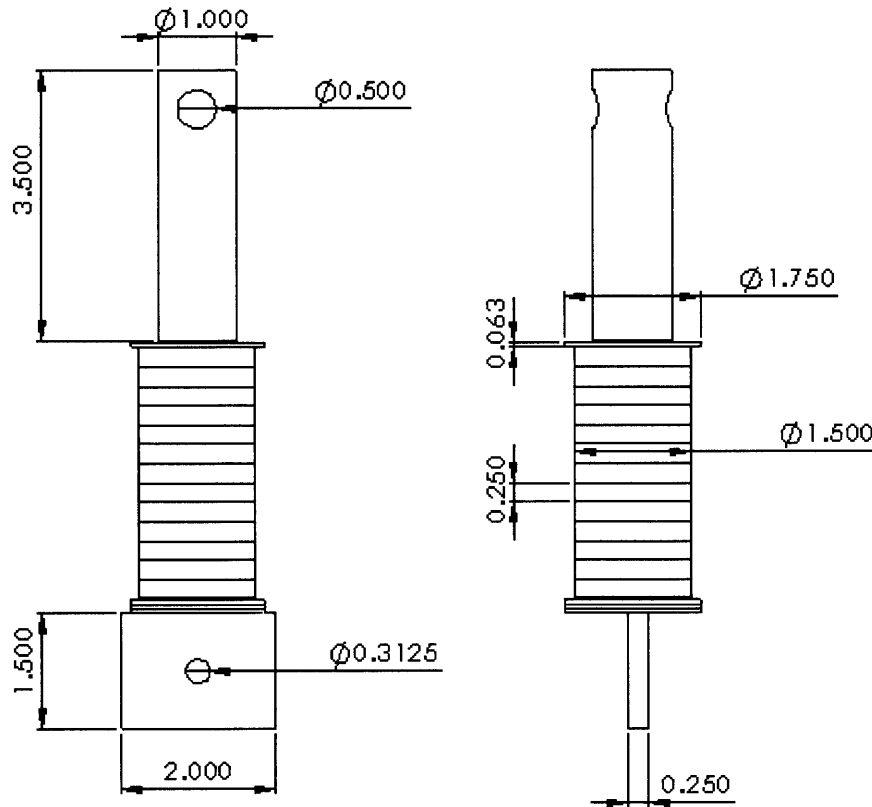


Figure A8: Dimensions of Spring Mount and Spring. The dimensions shown are in inches.

The washers separate the spring from the one inch tube and keep the tire rubber donuts from bowing around the bottom connection to the front wheel axle bar. These ought to have a greater outer diameter than that of the tire rubber donuts.

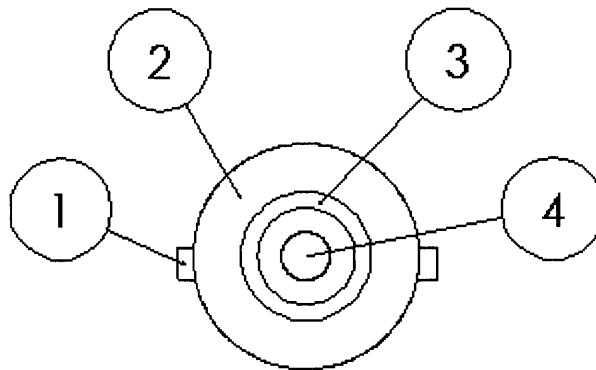


Figure A9: Spring Mount Viewed From Above. Several pieces of the spring mount can be seen when looking at the mount from directly overhead. They are (1) the rectangular bottom attachment, (2) a washer, (3) the piece of one inch tubing, and (4) the rod on which the spring is slid. The rod should be concentric with the one inch tubing during the suspension system's operation.

## Appendix B: Tire Rubber Donut Manufacturing Instructions

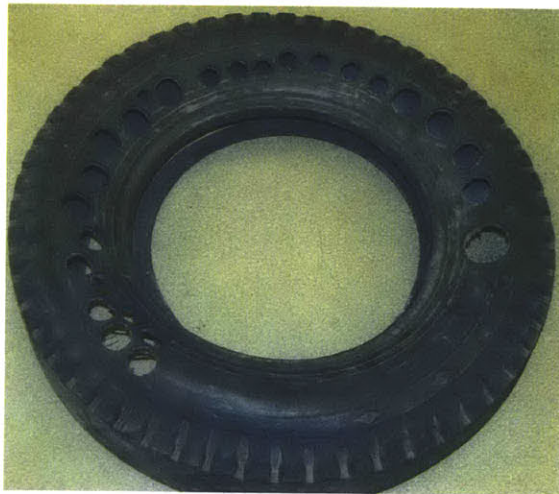
In order to create the tire rubber donuts necessary for the suspension system, a drill, a hole saw of the appropriate diameter, and a set of drill bits will be required.

1. Set drill to its lowest gear. A significant amount of torque is needed to cut through the ply.
2. Drill starter hole with any size drill bit. This drill bit should be roughly the same size as the one that is attached to the hole saw to be used.
3. Attach hole saw to drill and begin drilling hole.
4. Stop drilling hole half way through the tire sidewall.
5. Replace hole drill with  $\frac{25}{64}$  inch drill bit\*.
6. Drill out the starter hole. In order to get a better cut, pull the drill out of the hole while it is still running forward. Then, toggle the drill to run backwards while pushing it into the hole.
7. Replace drill bit with hole saw.
8. Finish drilling hole.

Notes: An exacto-knife may be needed to finish the cut.

Drill one donut that fits around the rod and inside of the tubing. This will prevent the rod from rubbing on the inside of the tube, thus decreasing wear and tear.

Neglecting steps 4-6 will create a hardship as it is very difficult to drill the starter hole out after the donut is no longer attached to the rest of the tire.



\* These directions are specifically for use to create donuts for 3/8 inch rod. If the rod is a different size, adjust this drill bit's size accordingly.

### Appendix C: From the Ground's Frame of Reference

Using the ground as a frame of reference, the entire rickshaw will pivot around the back wheel's contact with the ground when the front wheel goes over a bump.



Figure C1: Rickshaw With Ground-based Pivot. The Rickshaw Bank's rickshaw illustrates the distance between the pivot point and the location of the three points of interest on the beta-prototype.

The elements of the front suspension fork are experiencing forces at the pivot between the top link and the handlebar bar, the attachment point between the top link and the mount, and the pivot between the top link and the front wheel axle bar. The geometry to explain the location of these forces is shown in Figure C2.

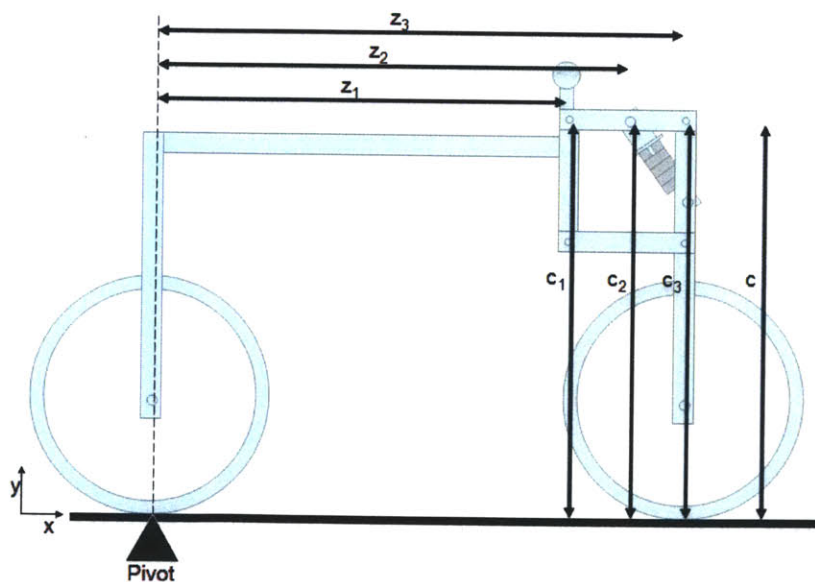


Figure C2: Distances From Pivot To Forces. These distances are the moment arms for each of the three points at which the forces of interest act. Before any external forces are applied, the height of the pivot between the handlebar bar and the top link  $c_1$  is the same as the height  $c$ .

At equilibrium, Equation (C1) is true.

$$\Sigma M = 0 = z_1 F_{1,y} + z_2 F_{2,y} + z_3 F_{3,y} + z_3 F_{N,y} + c_1 F_{1,x} + c_2 F_{2,x} + c_3 F_{3,x}, \quad (C1)$$

where  $\Sigma M$  is the summation of the moments,  $F_{i,y}$  is the portion of the force at point  $i$  that is perpendicular to moment arm  $z_i$ , and  $F_{i,x}$  is the portion of the force at point  $i$  that is perpendicular to the moment arm  $c_i$ .

The height of the handlebars  $c_l$  after an external force has been applied can then be calculated using Equation (C2).

$$c_1 = \frac{z_1 F_{1,y} + z_2 F_{2,y} + z_3 F_{3,y} + z_3 F_{N,y} + c_2 F_{2,x} + c_3 F_{3,x}}{-F_{1,x}} \quad (C2)$$

Therefore the handlebars will rise by  $c_l - c$  for a given force.

## Appendix D: MathCad Code




### System Identification Via FFT

Ian Hunter, MIT

#### Introduction

In previous notes we have discussed methods to estimate the impulse response function via Toeplitz matrix inversion. In these notes we outline a technique based on the fast Fourier transform (FFT) to estimate the frequency response function of a system.

Copy your data into the table below. First column is time (in s), second and third are the input and output amplitudes

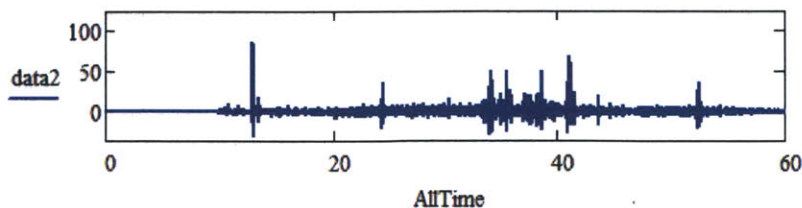
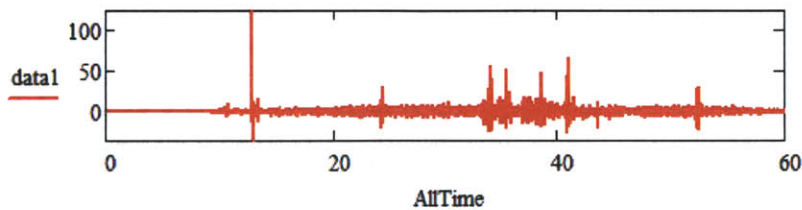
Data :=   
4-21 P1 t023 fft.csv

AllTime := Data<sup><0></sup>.s      data1 := Data<sup><1></sup>      data2 := Data<sup><2></sup>

$$\Delta t := \frac{\text{AllTime}_{100} - \text{AllTime}_0}{100} = 5 \times 10^{-3} \text{ s}$$

$$\text{SampleRate} := \frac{1}{\Delta t} = 200 \frac{1}{\text{s}}$$

$$\text{npts} := \text{length}(\text{AllTime}) = 11998$$



Define the "input" as x and the "output" as y from the data in the table above

x := data1

y := data2

For this sample, the column order was switched. You probably want x=data1, y=data2

### Compute the input power-spectrum

<pre> AutoSpectrum(x, m) :=   n ← length(x)   p ← n / m   for j ∈ 0..m/2     Sxmeanj ← 0     for k ∈ 0..p-1       for i ∈ 0..m-1         xx_i ← x_{i+m-k}         Sx ← ( fft(xx) )^2         for j ∈ 0..m/2           Sxmeanj ← Sxmeanj + Sx_j       for j ∈ 0..m/2         Sxmeanj ← Sxmeanj / p     return Sxmean </pre>	<p>Note that standard FFT algorithms (as used here) require that the data be a power of 2.</p> <p>we will split the input into p non-overlapping segments each of length N. (sometimes the successive segments are overlapped by as much as 50%)</p> <p>set the mean power spectrum to zero</p> <p>extract N length segment</p> <p>fast Fourier transform xx to get kth power spectrum</p> <p>add kth power spectrum to sum</p> <p>divide by p to get the mean power spectrum</p> <p>Note that p individual spectra have been averaged.</p>
--	---

N := 1024

Depending on your number of points, you may want to change this. It must be a power of 2. Higher number gives better frequency resolution at the expense of fewer samples to be averaged. You can vary it and look at the effect on the Bode plot to set it to the "best" value

p :=  $\frac{npts}{N}$

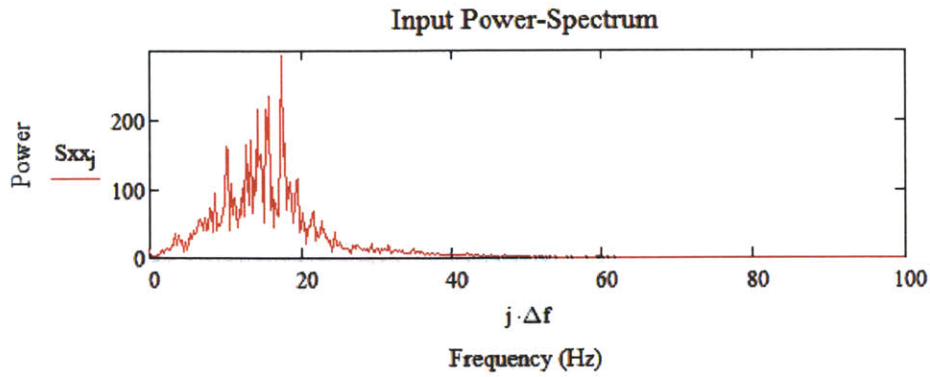
p = 11.717

p is the number of individual samples created from your data set and averaged

j := 0.. $\frac{N}{2}$      $\Delta f := \frac{1}{N \cdot \Delta t} = 0.195 \frac{1}{s}$     Hz

Remember that the frequency increment is the reciprocal of the duration of the signal which is taken here as the duration of the segment (i.e. m samples).

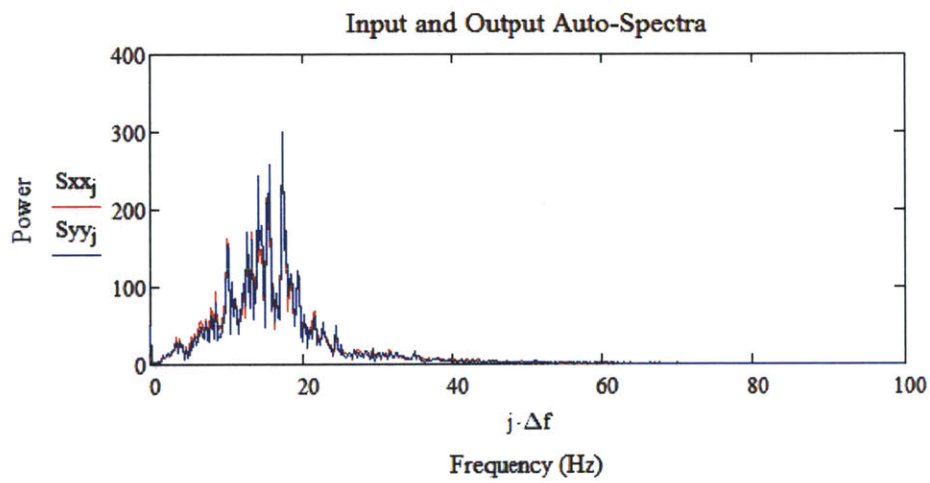
Sxx := AutoSpectrum(x, N)



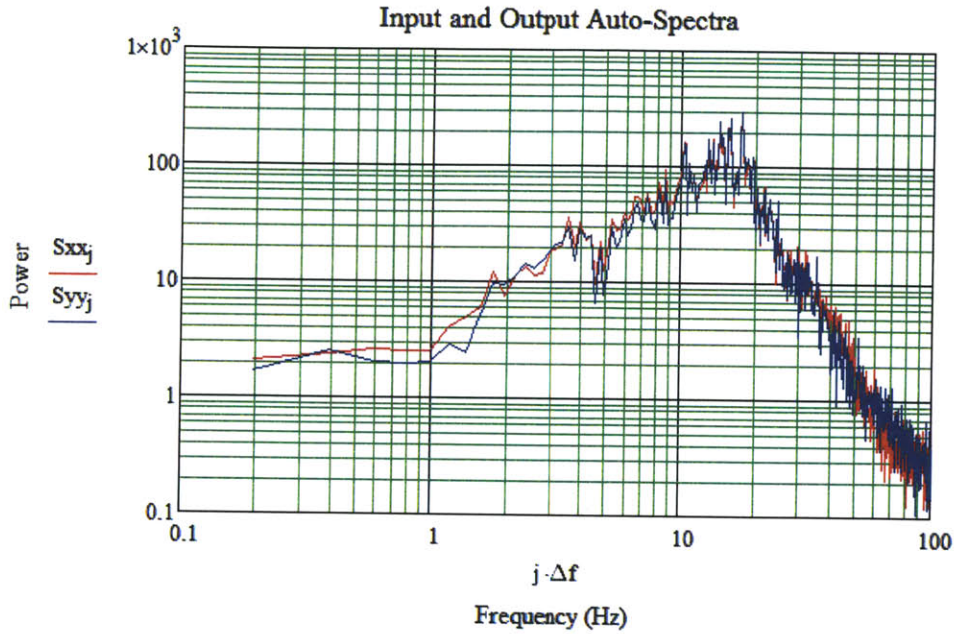
For white noise, this should be flat

Compute the output power-spectrum

```
Syy := AutoSpectrum(y, N)
```



It is more helpful to show the power-spectra on a log log plot



**Compute the input output cross-spectrum**

```

CrossSpectrum(x, y, m) :=
  n ← length(x)
  p ← n / m
  for j ∈ 0..m/2
    Sxymeanj ← 0
    for k ∈ 0..p-1
      for i ∈ 0..m-1
        | xxi ← xi+m·k
        | yyi ← yi+m·k
        Sxy ← (fft(xx) · conj(fft(yy)))
        for j ∈ 0..m/2
          Sxymeanj ← Sxymeanj + Sxyj
    for j ∈ 0..m/2
      Sxymeanj ← Sxymeanj / p
  return Sxymean

```

we will split the input into p non-overlapping segments each of length m. (sometimes the successive segments are overlapped by as much as 50%)

set the mean cross spectrum to zero

extract m length segments

fast Fourier transform xx and yy to get kth spectrum (the bar over fft(xx) denotes complex conjugate)

add kth cross spectrum to sum

divide by p to get mean spectrum



$$S_{xy} := \text{CrossSpectrum}(x, y, N)$$

Note that  $S_{xy}$  has complex values.

### Estimate the frequency response function

The frequency response function,  $H$ , may be estimated by dividing the input output cross-spectrum,  $S_{xy}$ , by the input power-spectrum,  $S_{xx}$ .

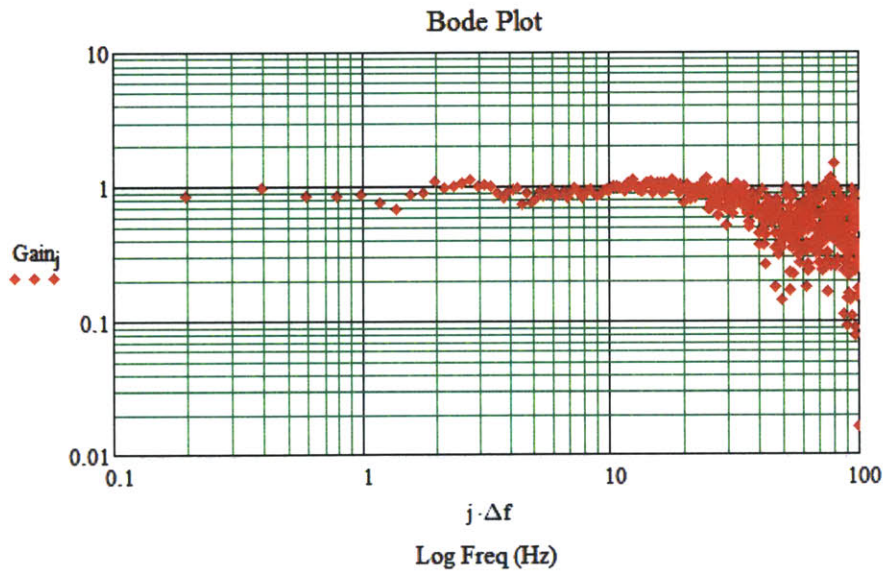
$$\underline{\underline{H}} := \left( \frac{S_{xy}}{S_{xx}} \right)$$

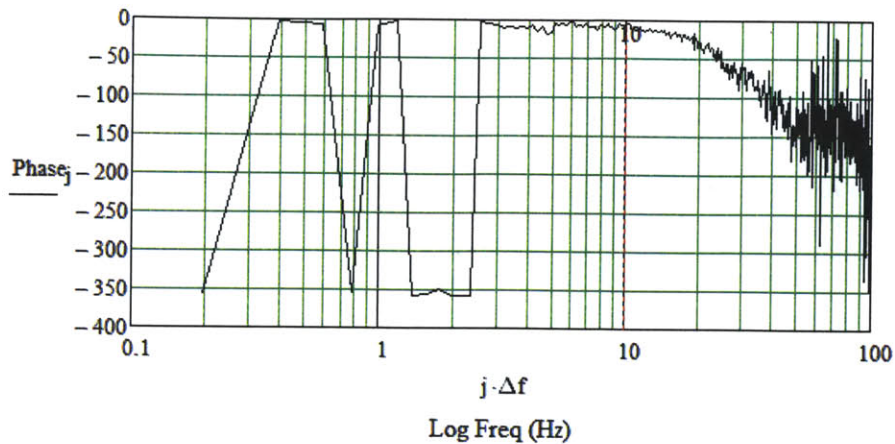
It is important to note that the power-spectrum is the Fourier transform of the auto-correlation function and the cross-spectrum is the Fourier transform of the cross-correlation function. Consequently this division of the input output cross-spectrum by the input power-spectrum is the frequency domain equivalent of deconvolving the input auto-correlation function from the input output cross-correlation function (e.g., via Toeplitz matrix inversion) in the time (or lag) domain.

$$\text{Gain} := |\underline{\underline{H}}|$$

$$\text{Phase} := -\text{angle}(\text{Re}(\underline{\underline{H}}), \text{Im}(\underline{\underline{H}})) \quad \underline{\underline{\text{Phase}}} := \text{Phase} \cdot \frac{180}{\pi}$$

The frequency response (Bode plots) is given by





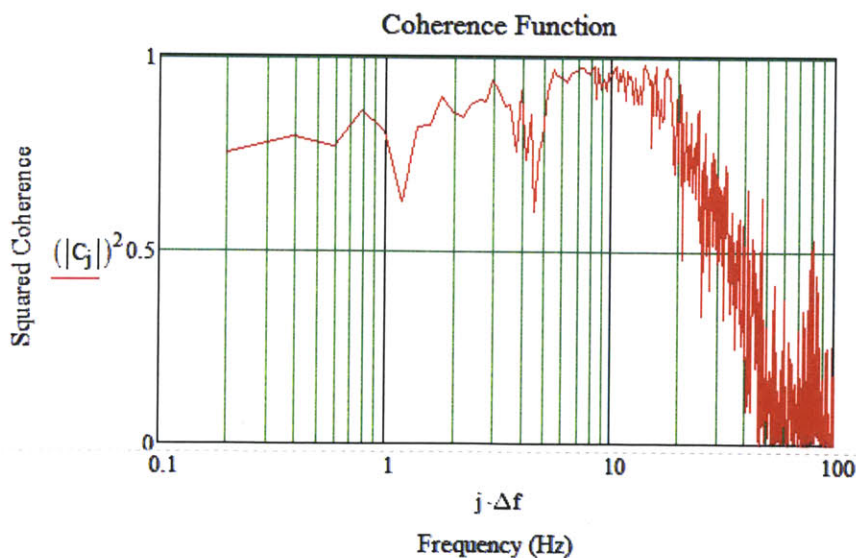
### Coherence Function

We need a measure of the degree to which we can have confidence in the estimates of the transfer function. A commonly used measure is the coherence function. The square of the coherence function value at each frequency is a measure of the output variance accounted for by the model (i.e. transfer function) at that frequency. In a sense the coherence squared function is a break down of the overall variance accounted for (%VAF) as a function of frequency. The coherence value at each frequency can be between 0 and 1. The coherence is high (near 1) when both the noise additive to the output is low and the system is linear. Conversely the coherence is low when there is significant noise and/or the system is nonlinear. It is important to note that with a nonlinear system the coherence function may be low even when there is no noise in the system.

The coherence function,  $H$ , may be estimated by

$$C_{\omega} := \left( \frac{\overline{S_{xy} \cdot S_{xy}}}{S_{xx} \cdot S_{yy}} \right)$$

We plot the coherence squared function:



We can see that in this case the coherence squared is low at high frequencies. This means that we have less confidence in our transfer function estimates at these higher frequencies. If a second-order transfer function (i.e. parametric model) is fitted to the measured transfer function (i.e. nonparametric frequency response model) using a least-squares objective function it is a good idea to weight the fit using the coherence values (i.e. weighted least-squares) in order to allow better transfer function estimates (i.e. having correspondingly higher coherence values) to have greater influence over the resulting parameter estimates.

In practice slow drift in systems can cause the coherence to be poor at low frequencies also.

## Appendix E: Additional Average Gain and $\phi$ Comparisons

### Varying Diameter

Varying diameter was shown to have basically no effect on the performance of the system in Section 6.2. This result was due to the impedance of the radial expansion caused by friction between individual tire rubber donuts and the effect of the number of embedded ply threads within each tire rubber donut.

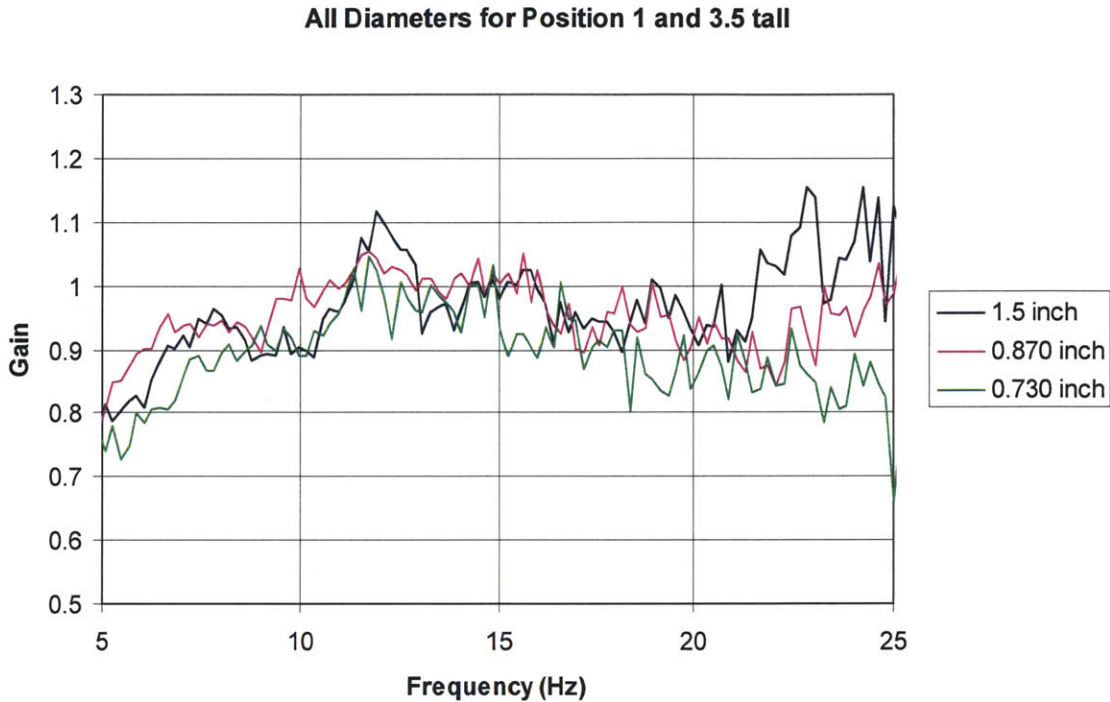


Figure E3: Varying Diameters. This graph is a closer look at frequency band that most affects the rickshaw drivers: 10-20 Hz. For these three configurations, the diameter was varied while the tire rubber donut stack measured 3.5 inches tall and the mount was held in Position 1.

Table E3: Figure of Merit for Varying Diameters. For these values of  $\phi$ , the diameter was varied while the tire rubber donut stack measured 3.5 inches tall and the mount was held in Position 1.

Diameter (inches)	$\Phi$
1.5	$0.98 \pm 0.01$
0.870	$0.98 \pm 0.01$
0.730	$0.94 \pm 0.02$

For the Figure E3 Bode Plot and these figures of merit shown in Table E3, the tire rubber donut stack was held at a constant length of 3.5 inches and the spring's mount was in Position 1. The diameter of the tire rubber donuts was varied. The system's performance with a diameter of 1.5 inches and with a diameter of 0.870 inches is almost indistinguishable. However, when the diameter is 0.730 inches, the systems performance is statistically significantly better than either of the other configurations.

### All Diameters for Position 3 and 3.5 Tall

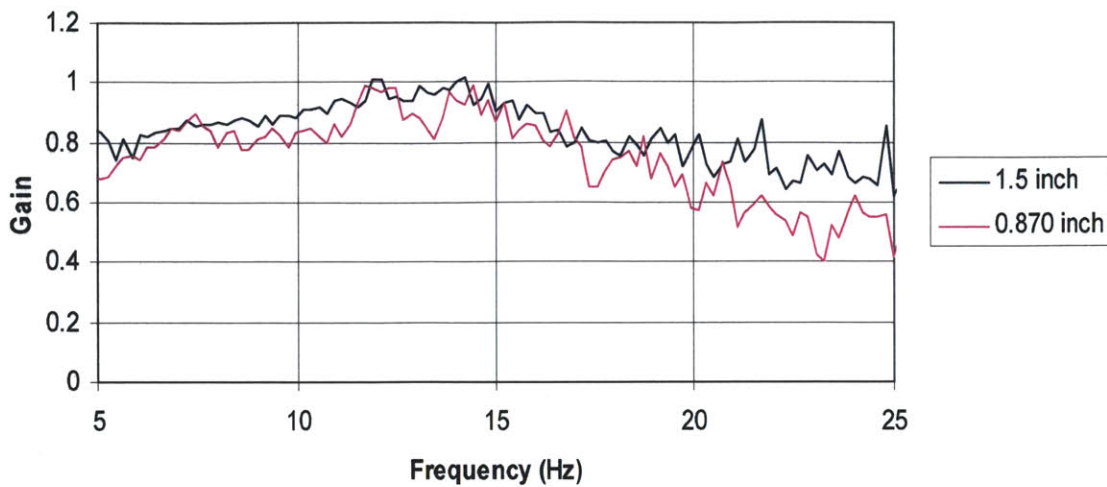


Figure E4: Varying Diameters. This graph is a closer look at frequency band that most affects the rickshaw drivers: 10-20 Hz. For these three configurations, the diameter was varied while the tire rubber donut stack measured 3.5 inches tall and the mount was held in Position 3.

Table E4: Figure of Merit for Varying Diameters. For these values of  $\phi$ , the diameter was varied while the tire rubber donut stack measured 3.5 inches tall and the mount was held in Position 3.

Diameter (inches)	$\phi$
1.5	$0.89 \pm 0.02$
0.870	$0.83 \pm 0.03$

The experimental data used to calculate the suspension system's response function shown in Figure E4 were taken from configurations where the length of the tire rubber stack was held at 3.5 inches and the mount was attached to Position 3 on the top link. Table E4 demonstrates that there is a discernible difference between the values of  $\phi$  for the two diameters shown. The configuration with the smaller diameter has a better system response. The configuration that used tire rubber donuts with a diameter of 0.730 inches is not shown here because it consistently bottomed out during testing. More information is available on that configuration and the effect of bottoming out on system performance in Figure 30.

### Varying Position

According to the information detailed in Section 6.2, position had the greatest impact on the system's performance. This can readily be seen in the response function shown in Figure E1. The geometry of Position 3, shown in Figure 19, gives it an advantage in terms of the angles it makes with the top link and with the front wheel axle bar.

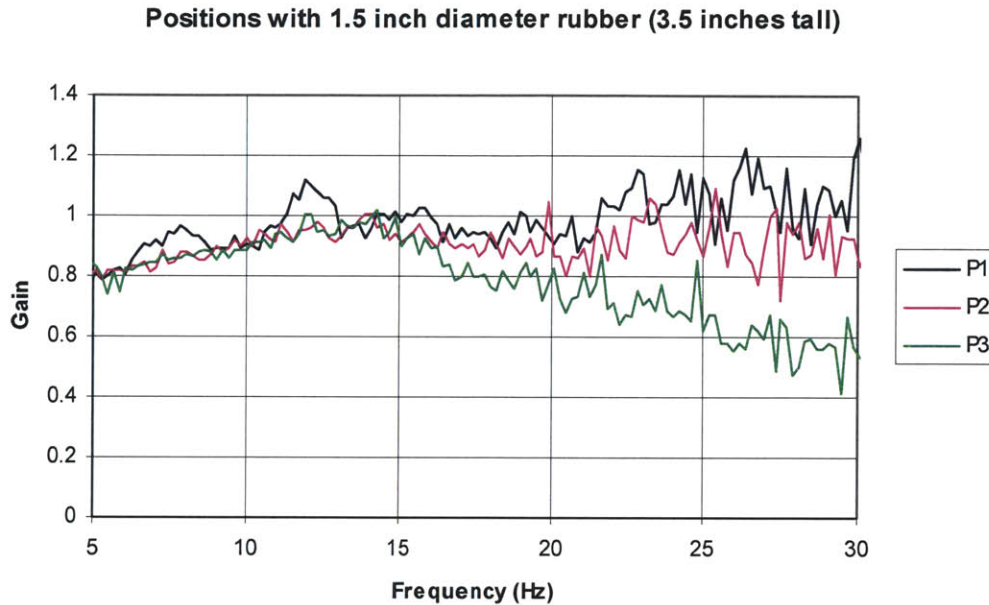


Figure E1: Varying Position. This graph is a closer look at frequency band that most affects the rickshaw drivers: 10-20 Hz. For these three configurations, tire rubber donuts with a diameter of 1.5 inches were placed in a stack measuring 3.5 inches.

Table E1: Figure of Merit for Varying Position. To calculate  $\phi$ , the diameter of the tire rubber donuts was held constant at 1.5 inches and the length of the tire rubber donut stack was also a constant of 3.5 inches.

Position	$\phi$
1	$0.98 \pm 0.01$
2	$0.93 \pm 0.01$
3	$0.89 \pm 0.02$

When varying position while holding the tire rubber diameter constant at 1.5 inches and stacked 3.5 inches tall, the value of  $\phi$  for each position does not overlap with the others, as seen in Table E1. Therefore, this trend serves as more evidence that as the moment arm increases, the effectiveness of the suspension system increases.

**Positions with 0.730 inch diameter (3.5 inches tall)**

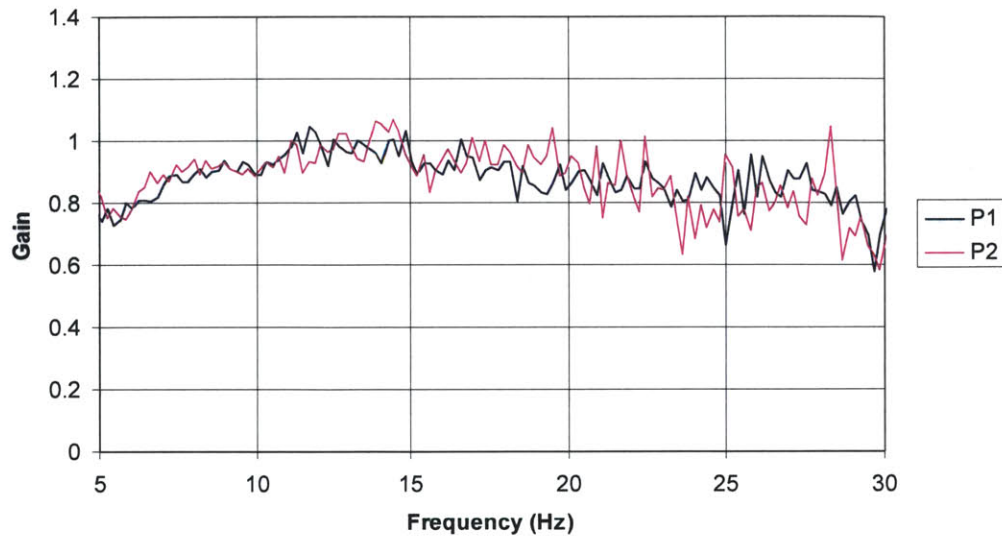


Figure E2: Varying Position. This graph is a closer look at frequency band that most affects the rickshaw drivers: 10-20 Hz. For these three configurations, tire rubber donuts with a diameter of 0.730 inches were placed in a stack measuring 3.5 inches.

Table E2: Figure of Merit for Varying Position. To calculate  $\phi$ , the diameter of the tire rubber donuts was held constant at 0.730 inches and the length of the tire rubber donut stack was also a constant of 3.5 inches.

Position	$\Phi$
1	$0.94 \pm 0.02$
2	$0.95 \pm 0.01$

For the configurations whose system response function and figure of merit are shown in Figure E2 and Table E2, respectively, position was varied while the tire rubber donuts with a diameter of 0.730 inches were placed in a stack 3.5 inches in length. The values of  $\phi$  for Positions 1 and 2 clearly overlap, much like they did for the configurations where the position was varied and the diameter was held at 0.870 inches. Position 3 is not shown here because that configuration bottomed out quite frequently. The average Bode Plot for that can be seen in detail in Figure 30.

## References

- [1] "Rickshaw Bank." *Centre for Rural Rural Development :: Ensuring Sustainable Development*. Centre For Rural Development. Web. 24 March 2011. <<http://www.crdev.org/rb.asp>>.
- [2] Ladd, Jeffrey. January 2010. Photograph. Guwahati, Assam, India.
- [3] Sarmah, Pradip. Personal interview. January 2010.
- [4] McDonald, Jeffrey A. Telephone interview. 23 April 2011.
- [5] Jazar, Reza N. "Chapter 1: Tire and Rim Fundamentals." *Vehicle Dynamics: Theory and Application*. New York, NY: Springer, 2008. 11-12. Print.
- [6] Duduk, Alexander. Radial, Bias Ply Tire. Robert Saifer, assignee. US Patent 3672423. 27 June 1972.
- [7] Ladd, Jeffrey. January 2010. Photograph. Guwahati, Assam, India.